UC San Diego
UC San Diego Electronic Theses and Dissertations

Title
Structural Studies on the MDM2-MDMX Heterodimer /

Permalink
https://escholarship.org/uc/item/3385w6jx

Author
Sano, Eleanor Shoko

Publication Date
2013

Peer reviewed|Thesis/dissertation

UNIVERSITY OF CALIFORNIA, SAN DIEGO

Structural Studies on the MDM2-MDMX Heterodimer

A thesis submitted in partial satisfaction of the requirements for the degree
Master of Science

in

Chemistry

by

Eleanor Shoko Sano

Committee in charge:

    Professor Hector Viadiu, Chair
    Professor Katja Lindenberg
    Professor Stanley Opella

2013

The Thesis of Eleanor Shoko Sano is approved and it is acceptable in quality and

form for publication on microfilm and electronically:

_____

_____

_____
Chair

University of California, San Diego

2013

TABLE OF CONTENTS

Introduction of MDM2 and MDMX

Purification and Expression of MDM2, MDMX, and the MDM2-MDMX

Heterodimer

LIST OF FIGURES

LIST OF TABLES

ACKNOWLEDGEMENTS

Before discussing the contents of this thesis, I would like to give thanks to the individuals who have greatly helped me during the past three years that I have worked in the research lab. First, I would like to express my gratitude towards Dr. Hector Viadiu. Not only did he provide guidance throughout my stay in the lab, but he also offered me an opportunity to do research despite my lack of experience as a lab worker. I sincerely believe that his keen observance, kindness, and open mind have helped bring the lab members closer together; thus, making the lab environment an amicable one.

Also, I appreciate Dr. Majid Ghassemian's help for taking my sample for Mass Spectrometry to validate the presence of MDM2 and MDMX. I would like to give a special thanks to Kate Kim and Nikki Cheung for providing me with the knowledge that was necessary to purify MDM2.

I would also like to show appreciation to the postdocs, Dr. Hiroyuki Akama and Dr. Abdul Ethayathulla, who never hesitated to help me when I needed it. I would also like to thank the lab members, Ana Ramos, Thien Nguyen, Frank Herkules, Kevin Lefever, Jill Tee-sy, Nhu-y Pham, and Jessie Wang, whom I have shared great memories with throughout the years. Without all of your support, I would not have been able pursue and obtain a master's degree. As for support outside of lab, I would like to show my gratitude to my family and friends, who have been there to for me in times of need anytime I needed it.

ABSTRACT OF THE THESIS

Structural Studies on the MDM2-MDMX Heterodimer

by

Eleanor Shoko Sano

Master of Science in Chemistry

University of California, San Diego, 2013

Professor Hector Viadiu, Chair

MDM2 is a protein that regulates p53 to prevent it from performing its tumor suppressor functions. In normal cells, MDM2 acts as an ubiquitin ligase to promote p53 degradation by attaching ubiquitin and sending it to the proteasome. MDMX is another negative p53 regulator that works in tandem with MDM2 by binding via their RING domains for dimerization. Studies have shown that MDM2

and MDMX are over-expressed in certain cancers, and are dependent of one another to function effectively as p53 regulators. Hence, the study of the MDM2-MDMX heterodimer is critical in anti-cancer research to provide more information on how it inactivates p53. By knowing the mechanism of p53 regulation, methods can be produced to inhibit MDM2 and MDMX activities and activate p53 functions for tumor suppression. However, the MDM2-MDMX heterodimer's structure has not been fully elucidated. The main objective of this thesis was the purification of the MDM2-MDMX complex and its subsequent 3D reconstruction using Electron Microscopy.

Chapter One

Introduction of MDM2 and MDMX

Although the p53 family members contain proteins that are significant to the pathogenesis of cancers and their mechanisms, MDM2 is also a protein that plays a significant role in cancer and in normal tissues as well. According to other studies, it has been determined that there is an amplification of MDM2 in many forms of tumors, including lung and stomach cancers (Toledo and Wahl, 2007). The amount of MDM2 expressed is directly proportional to the growth of tumors; hence, more tumor production equals to higher MDM2 expression levels (Toledo and Wahl, 2007). Even though there is an increase in MDM2 levels in some cancers, MDM2 also performs as regulators that inhibit p53 functions (Toledo and Wahl, 2007, Poyurovsky et al., 2007). Because of its regulatory properties, MDM2 is crucial in understanding cancer mechanisms and in developing anti-cancer drugs that could inactivate MDM2 to promote p53 activities.

Transcription Factors and Response Elements

Considering how p53 is a transcription factor, it is important to know what a transcription factor is. A transcription factor is an adaptor molecule that binds to certain DNA sequences to regulate gene expression (Zaret and Carroll, 2011). These DNA sequences (or response elements) are located within the gene's promoter region (Blanco et al., 2006, Wasserman and Fahl, 1997). The specificity of binding to response elements is critical; for example, p53 binds to specific sequences in the promoter region to activate tumor suppressor genes (Inga et al., 2002). Gene expression is performed via recruitment of RNA

polymerase ii for RNA synthesis (Figure 1.1) (Blanco et al., 2006). Besides inducing the transcription of genes, transcription factors are also able to initiate DNA repair (Zaret and Carroll, 2011). TFIIH is an example of a transcription factor that can induce DNA repair. Upon activation, TFIIH binds to another damage repair protein, Rad14, to create a repair complex at the damaged region, allowing NER (Nucleotide Excision Repair) to occur (Lommel et al., 2000). Although it depends on the molecules, transcription factors play a vital role in both protein synthesis and DNA repair.

The p53 Pathway and its Response to DNA Damage

In order to understand MDM2's involvement in the p53 pathway, it is pertinent to understand p53 and its own functions. Despite having p53 mutations in over 50% of cancers, p53 is still an essential tumor suppressor that responds to cellular stress (Bai and Zhu, 2006, Sakaguchi et al., 1998). Upon DNA damage, p53 expression is increased to promote apoptosis or cell cycle arrest to prevent genomic irregularities (Figure 1.2) (Bai and Zhu, 2006, Sakaguchi et al., 1998). These pathways are induced due to different post-translational modifications that p53 undergoes (Bai and Zhu, 2006). An example includes the involvement of ATM (Ataxia-Telangiectasia Mutated) and Chk2 to p53. When breaks are present in double-stranded DNA, both ATM and Chk2 are activated, which then phosphorylates p53 at specific sites to induce cell cycle arrest or apoptosis (Bai and Zhu, 2006). Since p53 is also a transcription factor, it also

has functions that induce gene expression. As a transcription factor, p53 induces p21 expression, which in turn initiates G1 cell cycle arrest (Bai and Zhu, 2006).

Introduction to MDM2 (Murine Double Minute 2)

MDM2 is a protein involved in many cancers, and is specifically involved in the regulation of the p53 pathway. MDM2 functions as an inhibitor of p53 and prevents it from being an effective tumor suppressor (Toledo and Wahl, 2007, Poyurovsky et al., 2007). MDM2 does so by acting as an E3 ubiquitin ligase to inhibit p53 (Cross et al., 2011). Although p53 is a tumor suppressor and MDM2 may seem to hinder p53's performance, it has been shown that MDM2 is still a necessary protein. Studies have presented that mice having a knockout of MDM2 experience embryonic death, supporting the idea that despite being a p53 inhibitor, MDM2 is still crucial in balancing out the life and death of an organism (Cross et al., 2011). Nonetheless, knowing and understanding the mechanism between MDM2 and p53 are necessary to understand the regulatory nature of MDM2.

MDM2's Regulation of p53

As mentioned earlier, MDM2 has a primary function of negatively regulating p53 in order to prevent p53 from performing its tumor suppressive functions. Upon cellular stress or DNA damage, tumor suppressor p53 is activated to initiate apoptosis or cell cycle arrest (Sasaki et al., 2011). However, p53 self-regulates by inducing MDM2 expression since MDM2 functions as an E3

ubiquitin ligase and promotes the degradation of p53; hence, creating a negative feedback loop between p53 and MDM2 (Rew et al., 2012, Sasaki et al., 2011).

Upon MDM2 interaction, p53 is transported from the cell's nucleus to the cytosol (Rew et al., 2012). Then, MDM2's E3 ligase properties allow ubiquitin's C-terminal region and the target protein's lysine to form a peptide linkage, ultimately leading the target protein out to the cytosol for proteosomal degradation (Fang et al., 1999, Sasaki et al., 2011). Besides being an E3 ubiquitin ligase, MDM2 has an alternative method of inhibiting p53. MDM2 is capable of binding to the p53 transactivation domain (TAD), rendering p53 incapable of performing target gene transcription (Rew et al., 2012). However, there are preventative methods to avoid MDM2-p53 interaction. Proteins such as ARF (Alternative Reading Frame) inhibit MDM2 from binding to p53, preventing MDM2 from degrading p53 (Deisenroth and Zhang, 2011). Nevertheless, MDM2 contains effective and efficient methods that allow it to be a potent p53 inhibitor. (Figure 1.3)

MDM2 Structure and Function

Like many other proteins, MDM2 consists of specific domains that function differently. Human MDM2 is a sequence containing 491 amino acids arranged in four core domains (Moll and Petrenko, 2003). These domains include the p53 binding domain, the central acidic domain, zinc finger domain, and the RING domain (Figure 1.4).

p53 Binding Domain

The p53 binding domain is at the N-terminal region and is located from residues 26 through 108 (Priest et al., 2010). This region consists of a deep, hydrophobic cleft that allows the interaction of MDM2 and p53 through each others' N-terminal domains (Chene, 2003, and Cross et al., 2011). Also, this domain is responsible for MDM2 binding to prevent p53 activation via proteasomal degradation (Priest et al., 2010). Hence, the p53 binding domain is crucial not only to repress p53 activities, but also to allow MDM2 to bind to p53 in order to function as an effective ubiquitin-ligase.

Central Acidic Domain

The central acidic domain is located from amino acid residues 230 to 274, and is a crucial portion for MDM2 function (Priest et al., 2010). The acidic domain participates in p53 inhibition by preventing DNA from binding to p53 by inducing p53 structural changes (Cross et al., 2011). This domain also contributes to p53 inhibition using alternative methods as well. It does so through posttranslational modifications, which include phosphorylation (Priest et al., 2010, Dias et al., 2009). Serine residues within the acidic domain can be phosphorylated to stimulate MDM2 activity (Dias et al., 2009). Other proteins also interact with the acidic domain to activate MDM2. These proteins include YY1 and p300. YY1 is a transcription factor and p300 is a transcription co-activator that are both capable of binding to the acidic region in order to activate MDM2's ability to ubiquitinate p53 (Dolezelova et al., 2012). However, not all

proteins promote p53 inhibition. Some proteins, such as ARF, are MDM2 inhibitors that prevent p53 from being degraded by binding to MDM2's central acidic domain (Cross et al., 2011). Hence, this region can serve as positive and negative regulators of MDM2 depending on its modification and interaction with other proteins.

Zinc Finger Domain

The zinc finger domain is positioned from amino acids 289 to 331, and is located after the central acidic domain (Priest et al., 2010). Although the exact functions of this domain are unclear, mutations in the zinc finger regions prevent MDM2 from acting as an effective p53 negative regulator (Lindstrom et al., 2007). Although wild-type MDM2 has the ability to export p53 to the cytosol for proteosomal degradation, a mutation in the zinc finger domain impairs this ability, despite still having the ability to debilitate p53 transcriptional performance (Lindstrom et al., 2007). The MDM2 zinc finger domain mutant also alters the interaction with other proteins as well. For example, the protein L11 inhibits wild-type MDM2's ability to suppress p53; however, L11 is incapable of stopping a MDM2 mutant from performing p53 suppressing functions (Lindstrom et al., 2007). Therefore, mutations in the zinc finger region detriment the MDM2's primary functions.

Really Interesting New Gene (RING) Domain

The Really Interesting New Gene (RING) domain is the last major domain that is located at the C-terminus (Priest et al., 2010). Residues 437 to 491 make up the domain, and it is capable of coordinating two zinc molecules with certain histidine or cysteine residues (Priest et al., 2010). Besides having the ability to bind zinc molecules to MDM2, the RING domain also serves other structural and functional purposes. The RING domain is crucial for MDM2 to perform as an E3 ubiquitin ligase, for that domain interacts with the E2 ubiquitin-conjugating enzyme to transfer ubiquitin for p53 degradation (Cross et al., 2011, Ranaweera and Yang, 2013). Not only is this domain important in ubiquitin ligase activity, but the RING domain also serves as a binding site to promote the formation of protein oligomers; thus, allowing MDM2 to form higher order oligomers (Priest et al., 2010).

MDMX and its interaction with MDM2

There are multiple types of proteins that serve as p53 regulators. Besides MDM2, Murine Double Minute 4 (also known as MDM4 or MDMX) is another negative p53 regulator (Wade et al., 2010). Although MDMX is a different protein, it does share many functional and structural qualities with MDM2. Like MDM2, MDMX is another necessary protein, for organisms lacking MDMX leads to p53-dependent lethality (Wade et al., 2010). Also similarly to MDM2, MDMX can thwart p53 activity and is frequently over-expressed in certain cancers (Wade et al., 2010). MDMX also has similar domains as MDM2, for they both have the p53 binding domain at the N-terminal region and a RING domain at the C-

terminal region (Wade et al., 2010). Despite their similarities, MDMX does have minute differences in terms of function. Unlike MDM2, MDMX does not function as an ubiquitin ligase, but instead, inactivates p53 via p53 TAD binding (Brooks and Gu, 2006, Wade et al., 2010). By binding to the p53 TAD, MDMX blocks a p53 alpha helix motif that is essential in gathering transcription activators to initiate transactivation (Wade et al., 2010). Therefore, MDMX acts as a negative regulator primarily through blocking p53's TAD.

Knowing that MDMX and MDM2 are both negative p53 regulators with structural and functional similarities, researchers have attempted to study the possible interaction between the two proteins. Studies have shown that MDMX and MDM2 can form heterodimers from binding via their respective RING domains (Tanimura et al., 1999, Wade et al., 2010). The reason for forming the heterodimer is possibly due to the stabilization of MDM2 and its amplification as an effective ubiquitin ligase (Huang et al., 2011, Pant et al., 2011, Tanimura et al., 1999). Considering how MDM2 itself is not as efficient in being an ubiquitin ligase, oligomer formation between MDM2 and MDMX is rather crucial (Huang et al., 2011). Hence, the study of the interaction between MDM2 and MDMX is essential in providing more information regarding p53 regulation.

Project Objective

The tumor suppressor protein p53 has been widely studied to gain more insight into its pathway and part in cancer. However, p53 regulation is necessary to retain functional stability, with MDM2 and MDMX being the primary regulators

(Francoz et al., 2006). Both MDM2 and MDMX are required in order for organism to avoid embryonic death from the over-expression of p53 (Cross et al., 2011). Hence, the involvement of MDM2 and MDMX is critical in survival even in normal tissues.

It has been claimed that MDM2 and MDMX function better as heterodimers as compared to homo-oligomers (Huang et al., 2011). Previous experiments show the functional differences between MDM2 as a monomer and as a hetero-complex with MDMX (Huang et al., 2011). Knowing that, scientists have tried, and succeeded in crystallizing a MDM2-MDMX heterodimer containing the RING domains (Linke et al., 2008). However, that is only the C-terminal region of the proteins, and the full length heterodimeric MDM2-MDMX structure has yet to be resolved.

This research partially focuses on the structural studies of the MDM2-MDMX heterodimer. By focusing on the MDM2-MDMX heterodimer, more structural and functional information about the regulators may be obtained. With that objective, structural reconstruction of the MDM2-MDMX complex was performed using electron microscopy.

The objectives of this project are:

I.   Co-expression and purification of MDM2, MDMX, and the MDM2-MDMX complex by using a vector containing multiple polylinker regions

II.   Analysis of the quaternary structure of MDM2, MDMX, and the MDM2-MDMX complex by using size-exclusion chromatography

III.   3D reconstruction of the MDM2-MDMX heterodimer by Electron Microscopy

a)
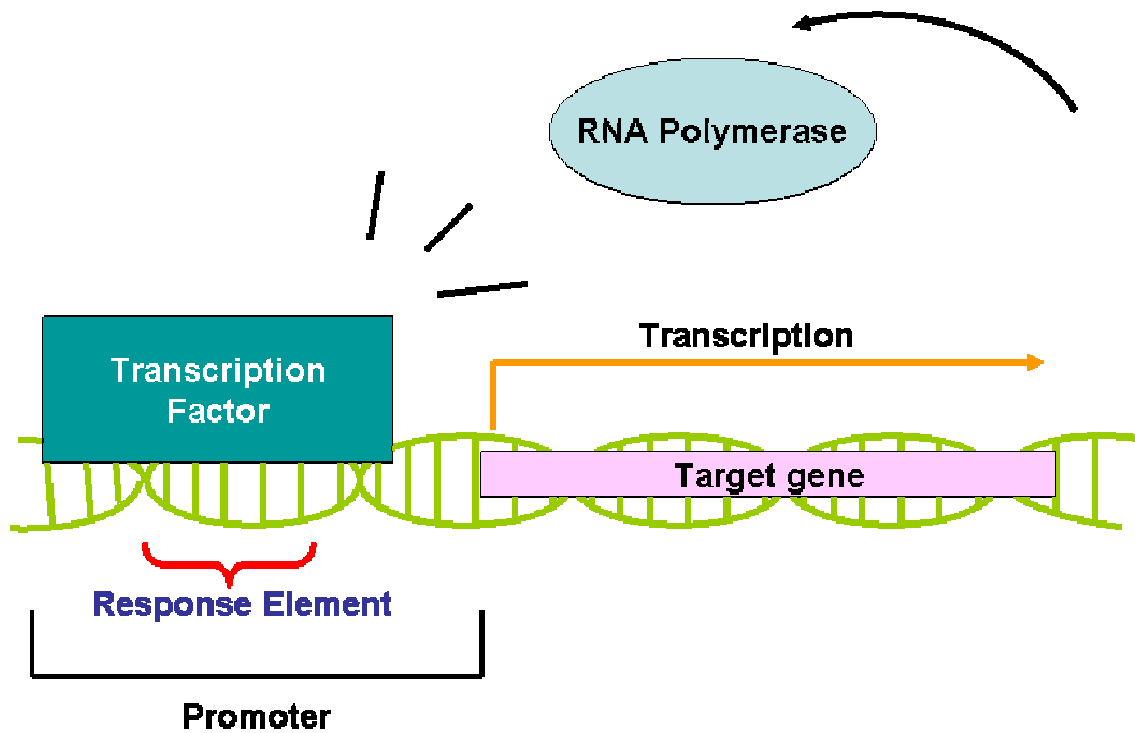
Figure 1.1. The Role of Transcription Factors. Transcriptions factors are composed of proteins that bind to response elements located in the promoter region of a target gene. Upon binding, the transcription factors recruit RNA polymerase to initiate gene expression.

Figure 1.2. The MDM2-p53 Pathway in Stressed Cells. In response to cellular stress or damage, p53 is activated to initiate cell cycle arrest, apoptosis, and other defense mechanisms. The negative regulator, MDM2, is inhibited by p53 activators. Both p63 and p73 are also transcription factors that are in the p53 family and act as tumor suppressors.

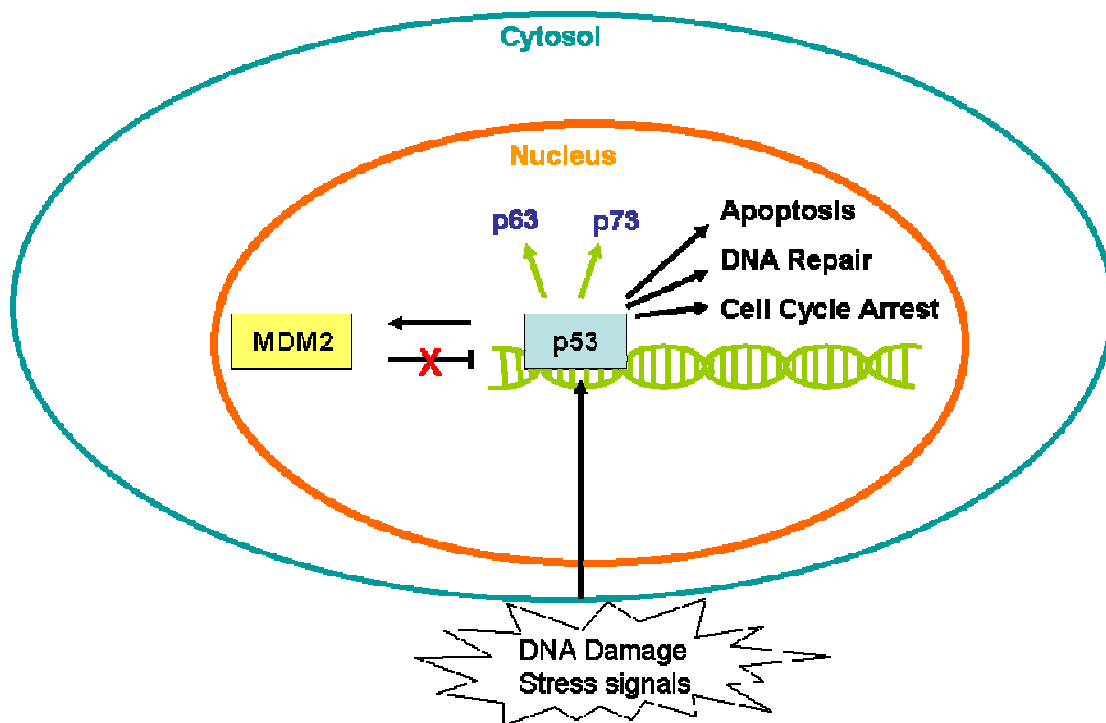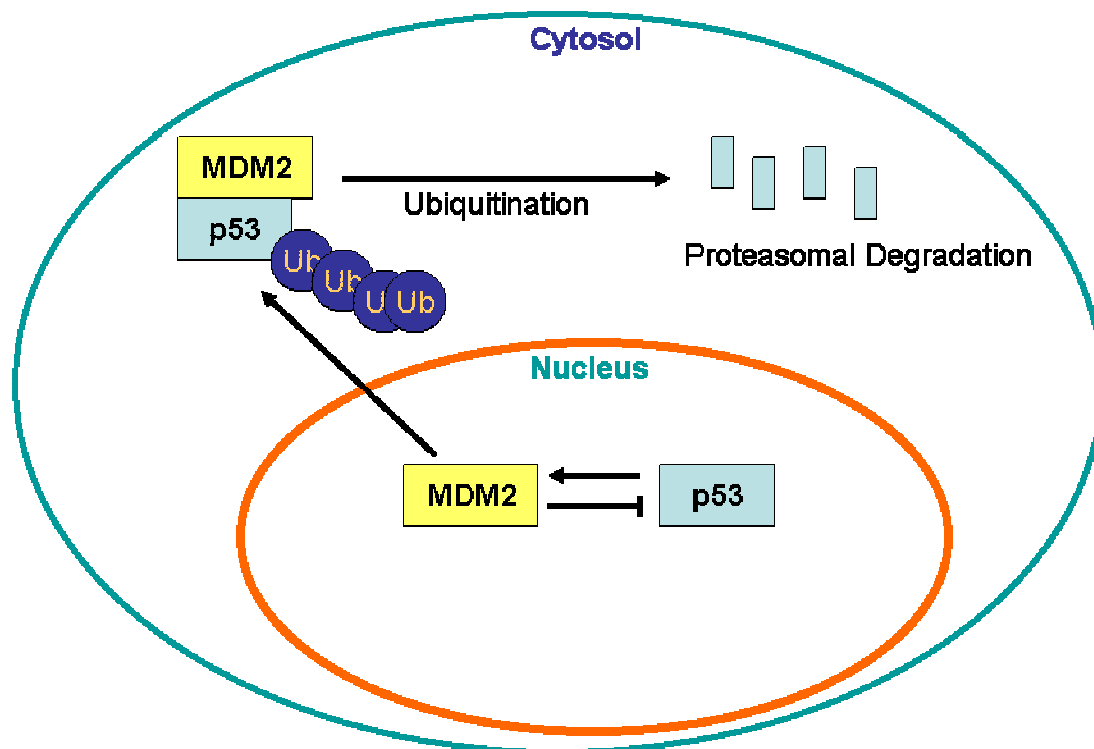**Figure 1.3. The MDM2-p53 Pathway in Normal Cells.** Under normal conditions, MDM2 regulates p53 by binding to p53's TAD. Once the MDM2-p53 complex is formed, it gets exported from the nucleus to the cytosol, where MDM2's E3 ubiquitin ligase activity promotes ubiquitin binding to p53. p53 is then sent to the proteasome for degradation. Proteins, such as ARF, are capable of preventing MDM2 from binding to p53; thus, allowing p53 to maintain its tumor suppressor functions (Deisenroth and Zhang, 2011).
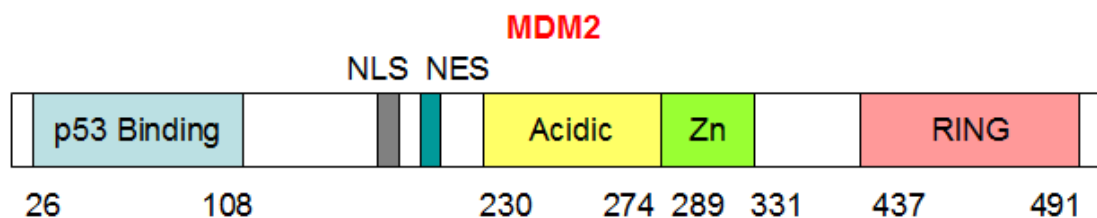
Figure 1.4. Human MDM2 Domains. MDM2 consists of 491 amino acids and contains the p53 Binding domain, Central Acidic Domain, Zinc finger domain, and the *Really Interesting New Gene* (RING) Domain. A Nuclear Localization Signal (NLS) and a Nuclear Export Signal (NES) is located between the p53 Binding domain and the Central Acidic domain.
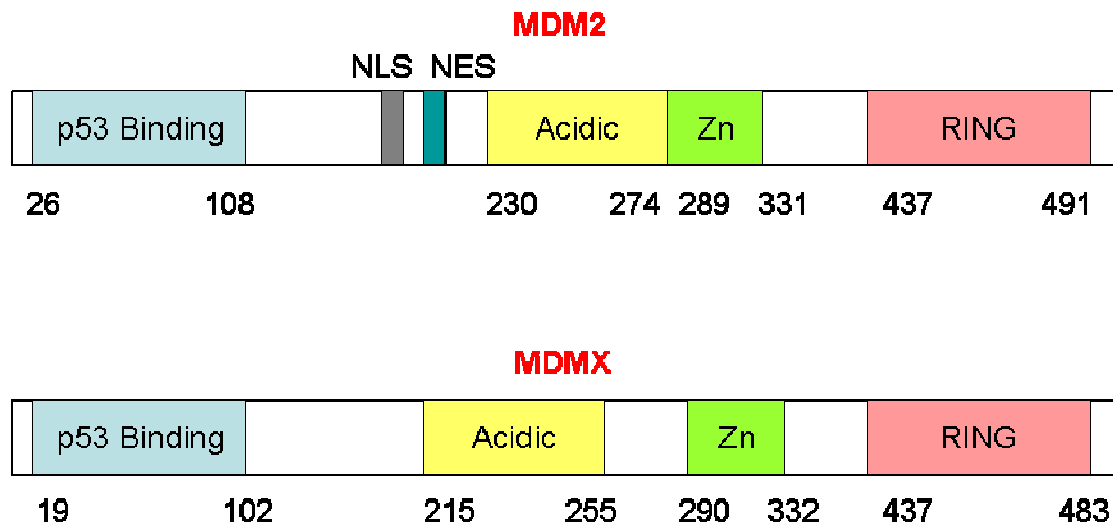
Figure 1.5. Domain Comparison of MDM2 and MDMX. Since MDMX is a homolog of MDM2, it consists of similar major domains. Both of the proteins contain the p53 binding, central acidic, zinc finger, and RING domains. According to the results from Tanimura et al., 1999, MDM2 and MDMX are thought to bind via their RING domains.

Chapter Two

Purification and Expression of MDM2, MDMX,

and the MDM2-MDMX Heterodimer

INTRODUCTION

MDM2 and MDMX are key regulators that affect the p53 pathway. The p53 pathway activates tumor suppressor activities that promote apoptosis or cell cycle arrest depending on the cellular stress signal (Stad et al., 2001). MDM2 and MDMX are both negative regulators that antagonize these p53 activities (Graves et al., 2012). While MDM2 functions as an E3 ubiquitin ligase to send p53 to the proteasome for degradation, MDMX thwarts p53 function by blocking the p53 TAD, and lacks ubiquitin ligase activity (Graves et al., 2012, Huang et al., 2011, Stad et al., 2001). Considering how MDM2 and MDMX are frequently over-expressed in certain cancers, cancer research promotes the production of MDM2 and MDMX inhibitors to aid in the prevention of p53 degradation (Graves et al., 2012, Melo and Eischen, 2012).

The two negative p53 regulators, MDM2 and MDMX, interact as a complex in order to carry out their functions. Both of these regulators share a common RING domain located at the C-terminal region (Graves et al., 2012). Through this domain, MDM2 and MDMX are able to bind together to form a heterodimeric complex (Huang et al., 2011, Graves et al., 2012). This interaction is initiated through certain post-translational modifications, such as phosphorylation, which promotes MDM2 and MDMX to be phosphorylated to signal their binding (Melo and Eischen, 2012). Their heterodimer is relevant in controlling the p53 mechanism, for it has been theorized that MDM2's ubiquitin ligase activity is more pronounced upon MDMX binding; hence, making the complex effective in degrading p53 (Graves et al., 2012).

Knowing that their interaction with each other is relevant in inhibiting p53 activity, the study of the MDM2 and MDMX complex is crucial for analysis. As mentioned before, a portion of cancer research has been concentrating on the interaction of p53 to the MDM2-MDMX complex in order to inhibit their anti-apoptotic functions in cancers (Melo and Eischen, 2012). Although this is the main goal of the research, since not many MDM2-MDMX structural data is available, the specifics of the heterodimer's functions still remain unclear (Graves et al., 2012). However, before structural data can be obtained, the MDM2 and MDMX complex must be successfully purified. This chapter focuses on the optimization of the purification protocol for the MDM2-MDMX heterodimer. Since previous experiments involving the individual expression and purification of MDM2 (The initial purification protocol for MDM2 was provided by Nikki Cheung and Sun Kyung Kim, Cheung, 2010, Kim, 2012) and MDMX have resulted in severe aggregation or contamination, attempts were made to try to purify the two proteins simultaneously. After separately expressing MDM2 and MDMX and subsequently co-purifying them, MDM2 and MDMX were expressed into a single vector for co-purification.

MATERIALS, METHODS, AND RESULTS FOR MDM2 AND MDMX

INDIVIDUAL EXPRESSION AND CO-PURIFICATION

Materials used for pET28 expression of MDM2 and MDMX

The expression vector pET28 was used to individually purify MDM2 (Cheung, 2010, Kim, 2012) and MDMX. The pET28-MDMX construct was created by using *EcoRI* and *HindIII* restriction enzymes to cut the vector. After MDMX gene insertion, the expression vector was subsequently ligated for transformation into *Escherichia coli (E. coli)* BL21 (DE3) cells. Since the MDM2 and MDMX genes were inserted into the region containing an N-terminal His-tag, Ni affinity chromatography was used for protein purification.

Method of individual expression and purification of each protein

MDM2 Expression and Purification (Cheung, 2010, Kim, 2012)

The pET-MDM2 cells were grown in Luria-Bertani (LB) media containing 30 µg/mL of kanamycin at 37 ℃. When the cell density reached an OD_{600nm} of 0.6-0.8, 0.5 mM isopropyl-1-thio-β-D-galactopyranoside (IPTG) was added for MDM2 expression. The cells were induced for 4 hours at 25 ℃. After induction, the cells were collected and centrifuged at 3500 RPM for 20 minutes. Once the cells were resuspended in lysis buffer (500 mM NaCl, 50 mM Tris (pH 8.0), 20 mM imidazole, 10 mM DTT), the French press was used to perform cell lysis. The resulting cell lysate was then subject to ultracentrifugation at 30,000 RPM for 30 minutes at 4 ℃. The supernatant from ultracentrifugation was then batch bound to Ni resin (approximately 1 mL per liter of cells) for Ni affinity

chromatography. After obtaining the flow through, the Ni column was washed with 100 mL of lysis buffer and 50 mL of 40 mM imidazole buffer (lysis buffer containing 40 mM of imidazole instead of 20 mM). A 100 mM to 500 mM imidazole buffer gradient was then used to elute the protein from the column (total of 25 mL of elution). The elutions were concentrated to 1 mL and injected into a size exclusion chromatography column (Superose6). An SDS-PAGE gel was run on the elutions to determine its purity. (Cheung, 2010, Kim, 2012)

MDMX Expression and Purification

After transforming the pET28-MDMX construct into *E. coli* cells, they were subsequently grown at 37 °C in LB media with 30 µg/mL of kanamycin. When the cell cultures reached a density of OD_{600nm} 0.6-0.8, 0.5 mM isopropyl-1-thio-β-D-galactopyranoside (IPTG) was added for gene induction. After induction, the cells were centrifuged for collection and purification. The cells were resuspended in lysis buffer (1 M NaCl, 50 mM Tris (pH 8.0), 20 mM imidazole, 10% glycerol) and homogenized for lysis. After lysing the cells using the French press, the lysate was ultracentrifuged at 30,000 RPM for 30 minutes. The supernatant was then batch bound to Ni resin (approximately 1 mL to one liter of cells). 100 mL of lysis buffer and 50 mL of 40 mM imidazole buffer (lysis buffer containing 40 mM imidazole) was passed through to wash the column. To elute the protein, a 100 mM to 500 mM imidazole buffer gradient was performed (25 mL of total elution). The elutions were then concentrated to 1 mL for injection into the Superose6 column.

Method of Co-purification of MDM2 and MDMX

The cells for pET28-MDM2 and pET28-MDMX were grown separately. 2 L worth of MDM2 cells were grown, while 1 L of MDMX cells was grown. After these cells were individually resuspended in lysis buffer (1 M NaCl, 50 mM Tris (pH 8.0), 20 mM imidazole, 10% glycerol), they were combined into a beaker for homogenization. Once the cells were homogenized, they were lysed using the French press. The MDM2-MDMX-combined cell lysate was then ultracentrifuged. The supernatant from the ultracentrifugation was incubated with Ni resin. After incubating the supernatant, the flow through from the Ni column was obtained. The Ni column was then washed with 100 mL of lysis buffer and 50 mL of 40 mM imidazole buffer (lysis buffer containing 40 mM imidazole). The protein was eluted using a 100 mM to 500 mM imidazole buffer gradient (25 mL). The elutions were then combined and concentrated for injection into the Superdex200 column for size exclusion chromatography. To assess the purity of co-purified MDM2-MDMX, a sample was used to run an SDS-PAGE gel.

Results from purifying MDM2 homo-oligomers

Using 1 M NaCl in the lysis buffer

MDM2 research has been done to determine the optimal purification protocol for pET28 MDM2. Based on the results of that research, the previous lysis buffer (500 mM NaCl, 50 mM Tris (pH 8.0), 20 mM imidazole) was changed. The initial lysis buffer resulted in low protein yield; therefore, changes were made

to create a more protein-soluble buffer. This was done by increasing the salt concentration from 500 mM to 1 M NaCl, and adding 10% glycerol into the buffer. When the 500 mM NaCl lysis buffer was used for cell lysis and Ni affinity chromatography, the elutions were subject to size exclusion chromatography. A comparison of the size exclusion chromatograms using 500 mM and 1 M NaCl can be seen in Figure 2.2. According to the chromatogram, using the 1 M NaCl buffer resulted in a peak production away from the void volume, indicating aggregation. Since the protein in the 500 mM NaCl prep mostly aggregated, 1 M NaCl was used for the rest of the experiments.

The purity of the elution (from the Ni column) was assessed using SDS-PAGE (Figure 2.1). The gel showed purified MDM2, but the elution was concentrated for further purification via size exclusion chromatography (using a Superose6 column). According to the size exclusion chromatogram, a broad peak was produced (Figure 2.2). That peak was collected for analysis using SDS-PAGE, which shows purified MDM2 with no contaminants (Figure 2.2).

Results from purifying MDMX homo-oligomers

After pET28 MDM2 purification was performed, purification of pET28 MDMX was done to determine its similarities or differences with MDM2. Figure 2.3 shows the SDS-PAGE gel of MDMX after it was eluted from the Ni affinity column. In comparison to the MDM2's Ni affinity elutions, the MDMX elution contains higher and lower molecular weight contaminants. To further purify the MDMX elutions, they were concentrated to 1 mL and injected into the Superose6

column for size exclusion chromatography. Like MDM2, MDMX also produced a broad peak, which was later collected for SDS-PAGE analysis (Figure 2.4). However, it can be seen that despite performing size exclusion chromatography, the MDMX fraction still contained many contaminants.

Results from Co-purifying MDM2 and MDMX

Prior research mentioned that MDM2 and MDMX form a complex that effectively regulates p53 (Huang et al., 2011). Believing that the MDM2-MDMX complex is more stable than the individual proteins, attempts were made to co-purify MDM2 and MDMX. Both pET28 MDM2 and pET28 MDMX's cells were grown separately. The cells were separately resuspended in lysis buffer. However, the resuspended cells (both containing MDM2 and MDMX) were combined and homogenized before cell lysis. After homogenization of the two proteins' cells, they were subsequently co-purified using Ni affinity chromatography and size exclusion chromatography. An SDS-PAGE gel of the Ni affinity elutions is shown in Figure 2.5. Compared to MDMX's elutions, co-purified MDM2-MDMX contained less contaminant proteins. The size exclusion chromatogram (using Superdex200) of the concentrated Ni affinity elutions is shown (Figure 2.6). Thyroglobulin, ferritin, and BSA were used as standards to determine the approximate location of the MDM2-MDMX heterodimer based on its molecular weight. According to the standards, the heterodimer should elute at ~61.0 minutes. However, no prominent peaks were present at that time.

Possible aggregation may have shifted the proteins to be eluted earlier (hence, the large peak at ~39.0 minutes is present).

MATERIALS, METHODS, AND RESULTS FOR THE CO-EXPRESSION AND PURIFICATION OF THE MDM2-MDMX COMPLEX

Materials for MDM2 and MDMX co-expression

The pETDUET vector was used for MDM2-MDMX co-expression since it contains two multiple cloning sites (MCS). The restriction enzymes *EcoRI* and *HindIII* were used to insert the MDMX gene, while *XhoI* and *NdeI* were used to insert the MDM2 gene.

Method for expression and purification of MDM2-MDMX

The recombinant plasmid was inserted and transformed into *E. coli* BL21 (DE3), which were then grown into Luria-Bertani (LB) as the growth medium. To avoid bacterial contamination, 100 μg/mL of ampicillin was added into 1 L of LB for cell growth. After growing at 37 ℃, the cell culture's OD_{600nm} was checked until it was between 0.6-0.8. Afterwards, 0.5 mM isopropyl-1-thio-β-D-galactopyranoside (IPTG) was added into each liter's worth of cells for overnight induction at 12 ℃. The cells were then centrifuged and the pellet was resuspended in lysis buffer (1 M NaCl, 50 mM Tris (pH 8.0), 20 mM imidazole, 10% glycerol). The microfluidizer was used for cell lysis and the resulting lysate was ultracentrifuged to separate the soluble and insoluble cellular components. Ultracentrifugation was performed at 4 ℃, 30,000 RPM for 30 minutes. The supernatant was then bound with Ni resin (1 mL per 1 L of cells grown) and batch bound for 1 hour in a 4 ℃ room. After batch binding, the resin-bound supernatant was passed through a gravity column. Once the supernatant

passed through the resin, it was then washed with 100 mL of lysis buffer (1 M NaCl, 50 mM Tris (pH 8.0), 20 mM imidazole, 10% glycerol). The resin was then washed with 75 mL of 40 mM imidazole buffer (1 M NaCl, 50 mM Tris (pH 8.0), 40 mM imidazole, 10% glycerol). A total of 25 mL of protein elution was obtained after an imidazole gradient elution (100 mM – 500 mM imidazole in 1 M NaCl buffer in 5 mL increments) was performed. The elution was then concentrated to 1 mL using an Amicon 10k concentrator and then loaded onto a Superdex200 size exclusion column using a different buffer (1 M NaCl, 50 mM Tris (pH 8.0), 10% glycerol, 0.2 mM $ZnCl_2$). The different purification steps involved for this protein were analyzed using SDS-PAGE and the Western Blot.

Results from Co-expression of MDM2 and MDMX and Optimization

Using the Peristaltic Pump versus the Batch Binding Method for Ni Affinity Chromatography

Many attempts were made to purify co-expressed MDM2-MDMX using a peristaltic pump, which was used to wash the Ni resin and to elute the protein before subjecting it to size exclusion chromatography. Since the peristaltic pump is an automated system that pushes solutions in the Ni resin cartridge, it was assumed that it would create more aggregates than the batch binding method. This was hypothesized when multiple protein purification preparationss were done using the peristaltic pump (Figure 2.7). Even though size exclusion chromatography was used to observe the quaternary structure of MDM2-MDMX, the results varied greatly (Figure 2.7). While some preps seemed to produce the

MDM2-MDMX heterodimer, others formed aggregates instead. In order to alleviate the aggregation problem, β-mercaptoethanol (β-me) was added into the buffers to prevent the formation of soluble aggregates. A new lysis buffer containing 10 mM β-me was created, and two purification preparations were repeated, comparing the usage of a peristaltic pump and a gravity column. Based on Figure 2.7, the β-me seemed to have partially alleviated the aggregation. However, the results from the Superdex200 have shown that even with the addition of β-me, the batch binding method produces a higher protein yield. Therefore, it was decided that β-me would be added to the buffers and the batch binding method would be used for Ni affinity chromatography.

Washes using a low salt buffer

In order to lessen the amount of contaminants bound to the Ni resin during affinity chromatography, the wash protocol was changed to incorporate a low salt buffer. Before, two 1 M NaCl buffer washes were done before the protein was eluted. The washes involved washing the resin with 100 mL of lysis buffer and then with 50 mL of 40 mM imidazole buffer (Figure 2.8). To try to rid the resin of more contaminants, the wash buffer was changed to a low salt buffer (50 mM NaCl, 50 mM Tris (pH 8.0), 20 mM imidazole, 10 mM β-me, and 10% glycerol). The new 40 mM imidazole buffer also contained 50 mM NaCl instead of 1 M NaCl to stay consistent. The imidazole elution buffers were kept at 1 M NaCl, and the subsequent elutions were injected into a Superdex200 column. According to the chromatogram and the SDS-PAGE gel of the collected elution

(Figure 2.9), there were less contaminants in the sample. To further purify the proteins complex, the purification protocol was changed to include three washes instead of two. The three washes involved washing the resin with 100 mL of 50 mM NaCl buffer, 75 mL of low salt, 40 mM imidazole buffer, and 50 mL of 50 mM NaCl buffer. The subsequent size exclusion chromatogram and SDS-PAGE gel of that protein sample is shown in Figure 2.10. According to the gel and the western blot, a relatively pure sample of MDM2-MDMX complex was obtained. Knowing this, an optimized purification protocol was produced (Figure 2.11) to obtain purified MDM2-MDMX heterodimer.

Validation of MDM2's and MDMX's presence

After purification via size exclusion chromatography, the protein sample (from Figure 2.10) was analyzed to confirm the presence of MDM2 and MDMX. A western blot using the His antibody was used to assess MDMX's presence, since MDMX was inserted into a multiple cloning site containing a His-tag (Figure 2.12). To check for MDM2, MDM2 antibodies were ordered to run western blots. The MDM2 N-20, SMP-14, and C-18 antibodies represent antibodies that bind to different MDM2 regions. According to the western blots, all of the antibodies developed signal, signifying the presence of MDM2 in the sample.

To further confirm MDM2's presence, a sample of MDM2-MDMX-p53 (when an attempt was made to purify the p53-MDM2-MDMX complex) was also sent to Dr. Majid Ghassemian for analysis via Electrospray Ionization (ESI) Mass

Spectrometry. According to the results shown in Table 2.1, MDM2 is present in the sample.
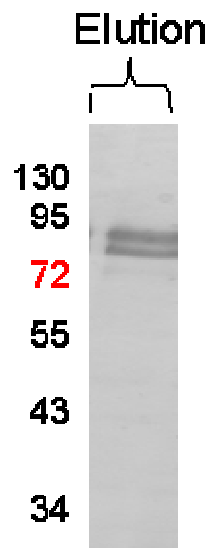
Figure 2.1. SDS-PAGE of MDM2 After Ni Affinity Chromatography. A gel was run on the elution after the protein was eluted using imidazole.   According to the gel, the elution consists of fairly pure protein.   Even though the molecular weight of MDM2 is ~56 kDa, the protein always appears at a higher molecular weight (between ~80 kDa to 95 kDa).
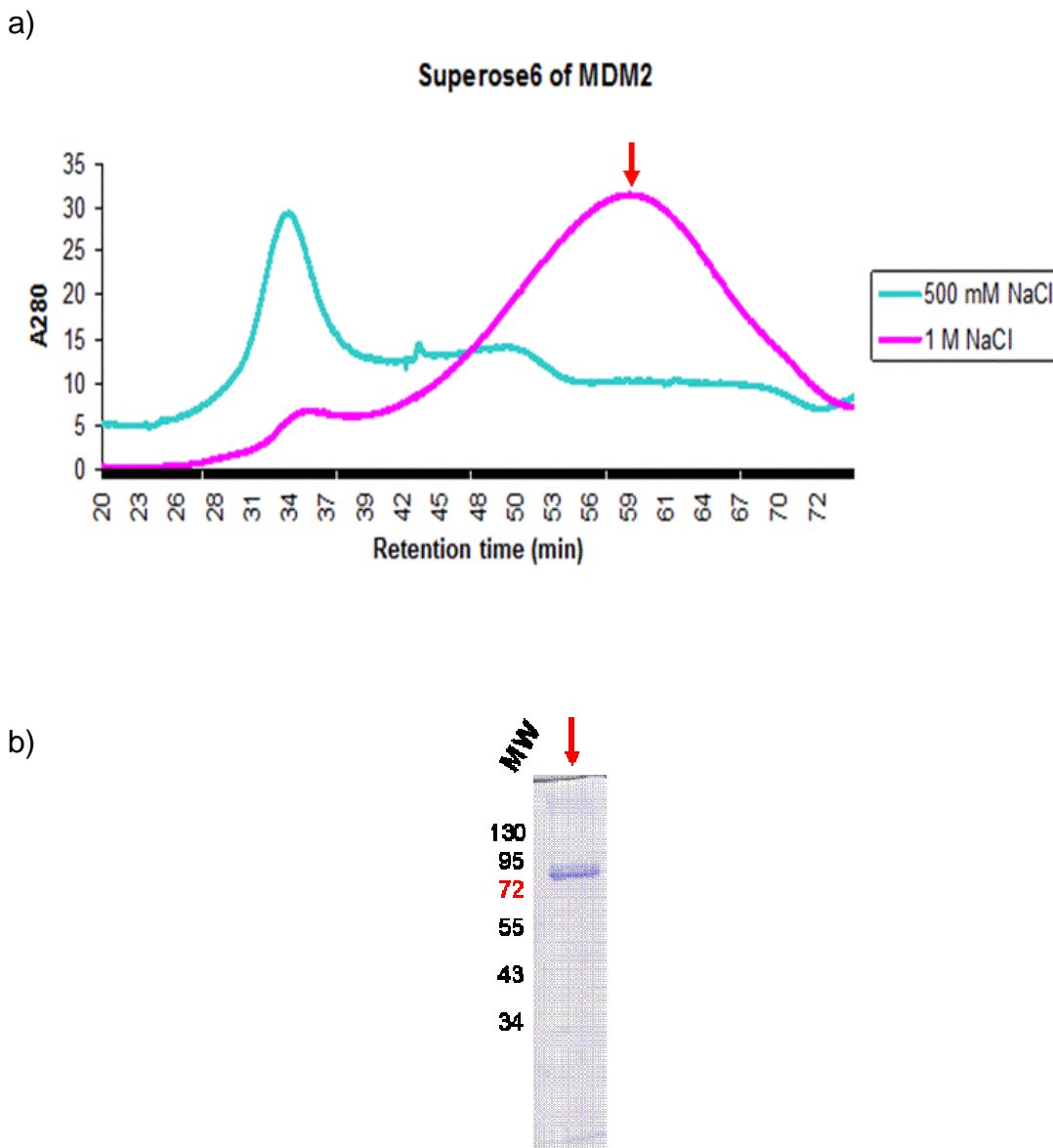
a)

b)

Figure 2.2. Chromatogram and SDS-PAGE gel of MDM2. A) To further purify MDM2, the elutions (from affinity chromatography) were concentrated to 1 mL and injected into a Superose6 column for size exclusion chromatography. A comparison of the chromatograms using 500 mM NaCl and 1 M NaCl in the buffers is shown. While a broad peak was produced for the prep containing 1 M NaCl, the prep with 500 mM NaCl produced a peak in the aggregate volume. The red arrow signifies the broad peak that was concentrated. B) An SDS-PAGE gel was run after combining the elutions contained in the broad (red arrow) peak in the chromatogram. According to the gel, the MDM2 sample seems devoid of higher or lower weight contaminants.
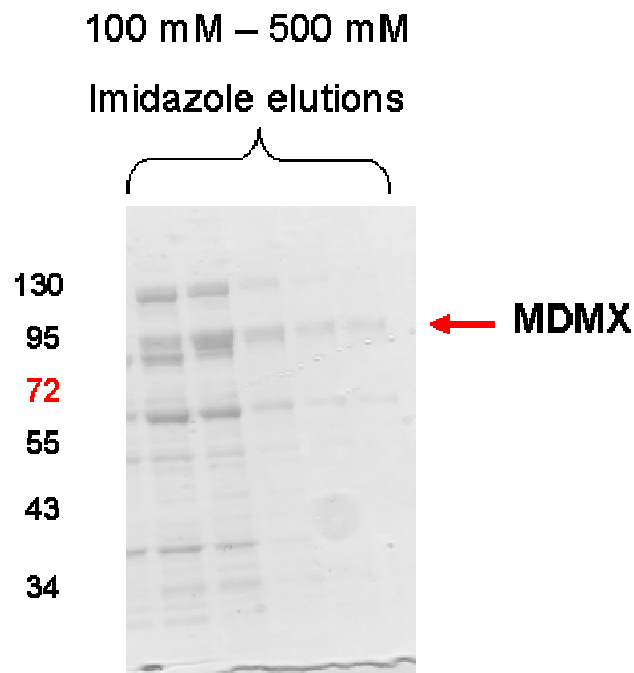
Figure 2.3. SDS-PAGE of MDMX After Ni Affinity Chromatography. The Ni affinity chromatography elutions are shown in the image above. MDMX was eluted from the Ni column using an imidazole gradient elution (100 mM to 500 mM imidazole). The red arrows points to the region where MDMX should be present. Unlike MDM2, MDMX contains higher and lower molecular weight contaminants.
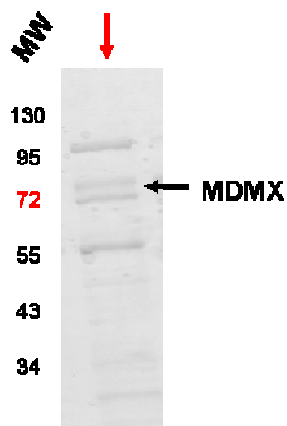
a)
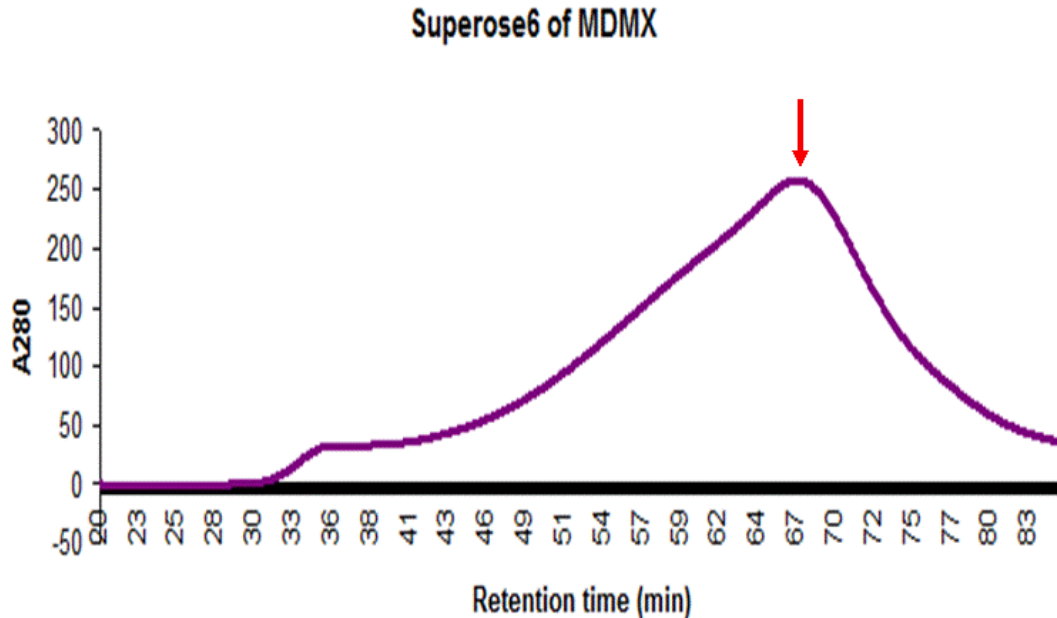
b)

Figure 2.4. Chromatogram and SDS-PAGE gel of MDMX. A) Like MDM2, MDMX also produced a broad peak after the elutions were collected and put through size exclusion chromatography. The red-arrowed peak was collected to asses its purity using SDS-PAGE. B) The elutions from the broad peak were collected and subject to gel electrophoresis to assess its purity. According to the gel, MDMX was present along with many contaminants.
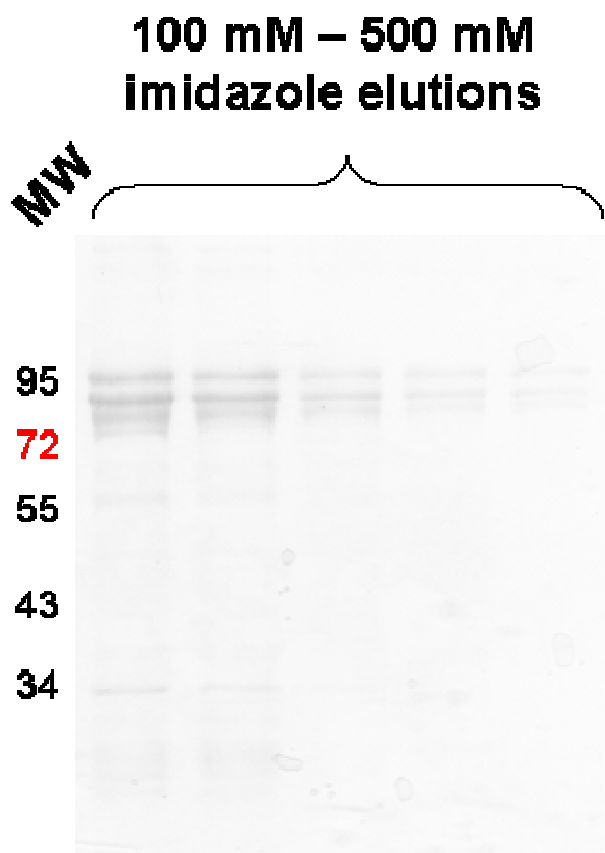
Figure 2.5. SDS-PAGE of Co-purified MDM2 and MDMX After Ni Affinity Chromatography. The gel above shows the imidazole elutions of the proteins after Ni affinity chromatography. In comparison to MDMX, the co-purified MDM2 and MDMX contained less contaminants. To further purify them, these elutions were combined and concentrated for size exclusion chromatography.
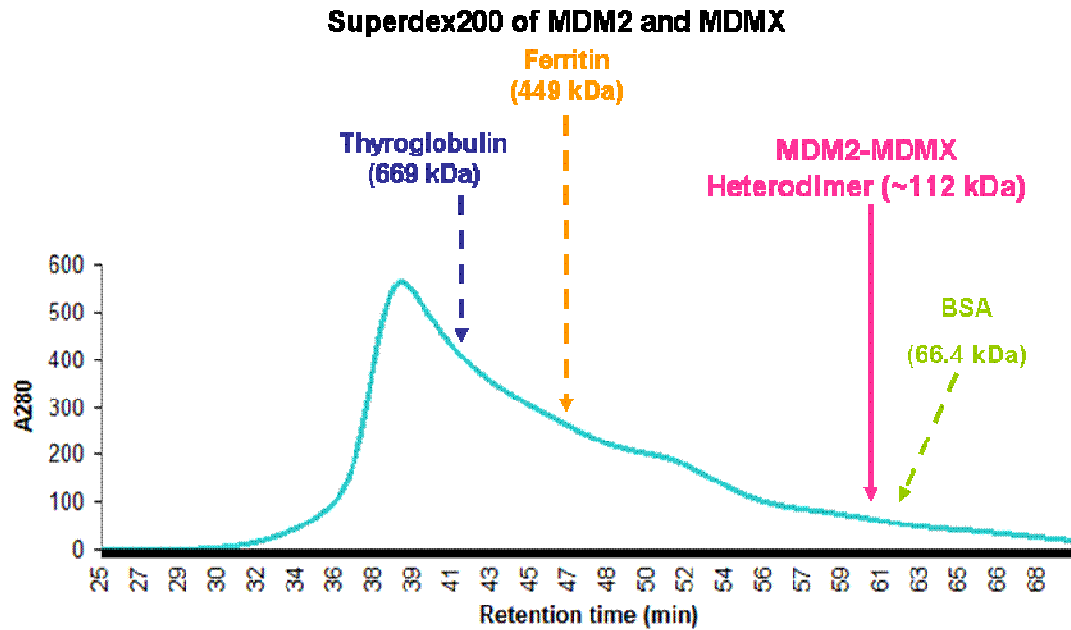
Figure 2.6. Chromatogram of MDM2 and MDMX During Co-purification.
After MDM2 and MDMX cells were grown separately, they were each
resuspended in lysis buffer to prepare for cell lysis. However, before cell lysis
was performed, the resuspended MDM2 and MDMX cells were combined and
homogenized together. The mixture was then lysed to begin MDM2-MDMX co-
purification. After Ni affinity chromatography, the MDM2-MDMX elution was
concentrated for size exclusion chromatography. In the chromatogram above,
the Superdex200's standards (Thyroglobulin, ferritin, and BSA) are shown along
with the approximate location/time when the MDM2-MDMX heterodimer should
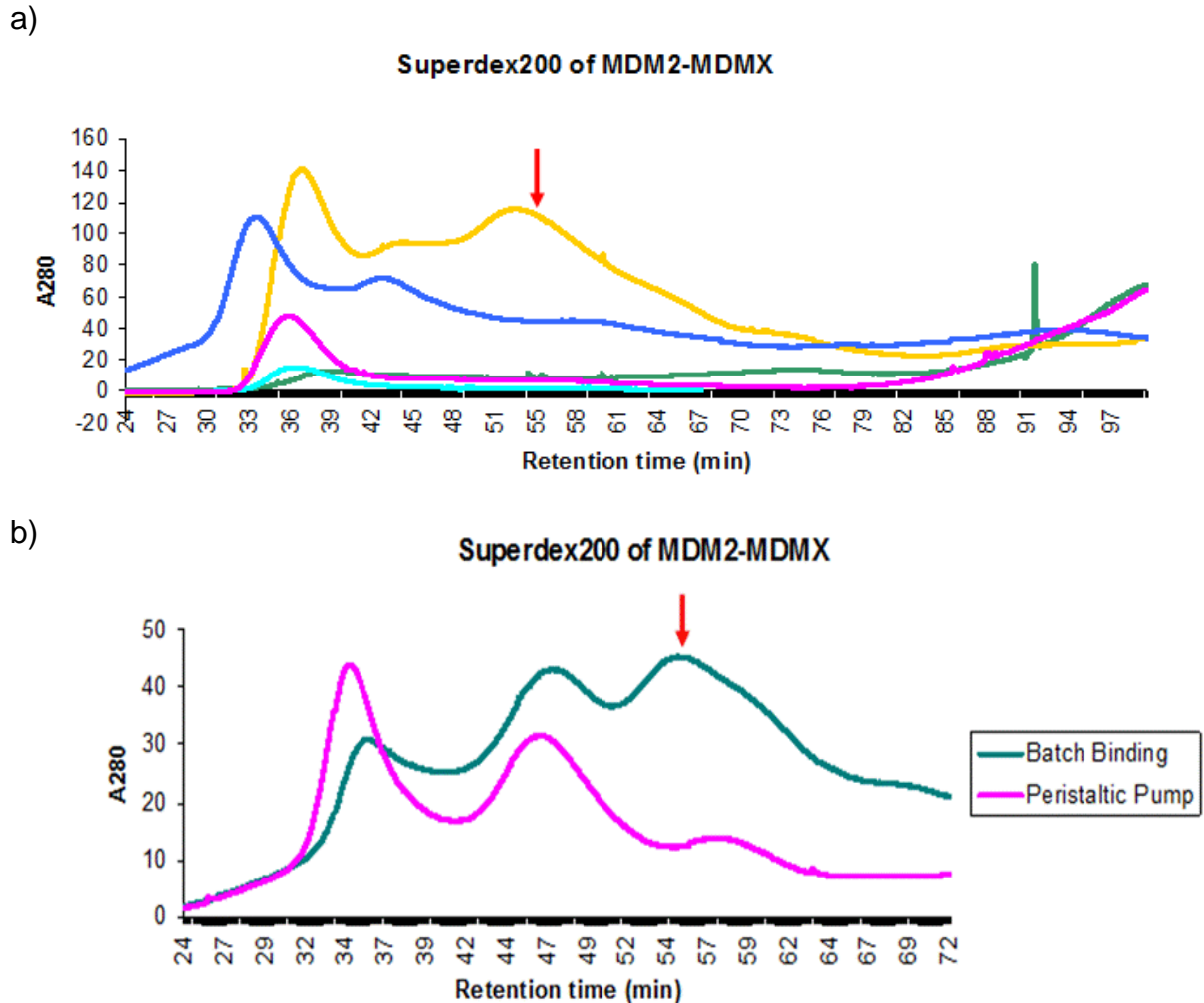elute. However, no distinct peak is shown in the approximate region.

a)

b)

Figure 2.7.   Co-expressed MDM2-MDMX Ni Affinity Chromatography: Peristaltic Pump versus Batch Binding. A) The graph shows the comparison of the Superdex200 chromatograms between the different preps using a peristaltic pump when performing Ni affinity chromatography. The red arrow shows the approximate location of the MDM2-MDMX heterodimer. It can be observed that the results obtained for the different peristaltic pump preps were inconsistent, and much of the protein complex has aggregated.   B)   This chromatogram compares the use of a batch binding column and a peristaltic pump for Ni affinity chromatography.   For both of the preps, β-me was incorporated into the buffers to alleviate the aggregation. Although the reducing agent partially helped with the aggregation, the batch binding prep showed a much higher yield than the peristaltic pump prep.
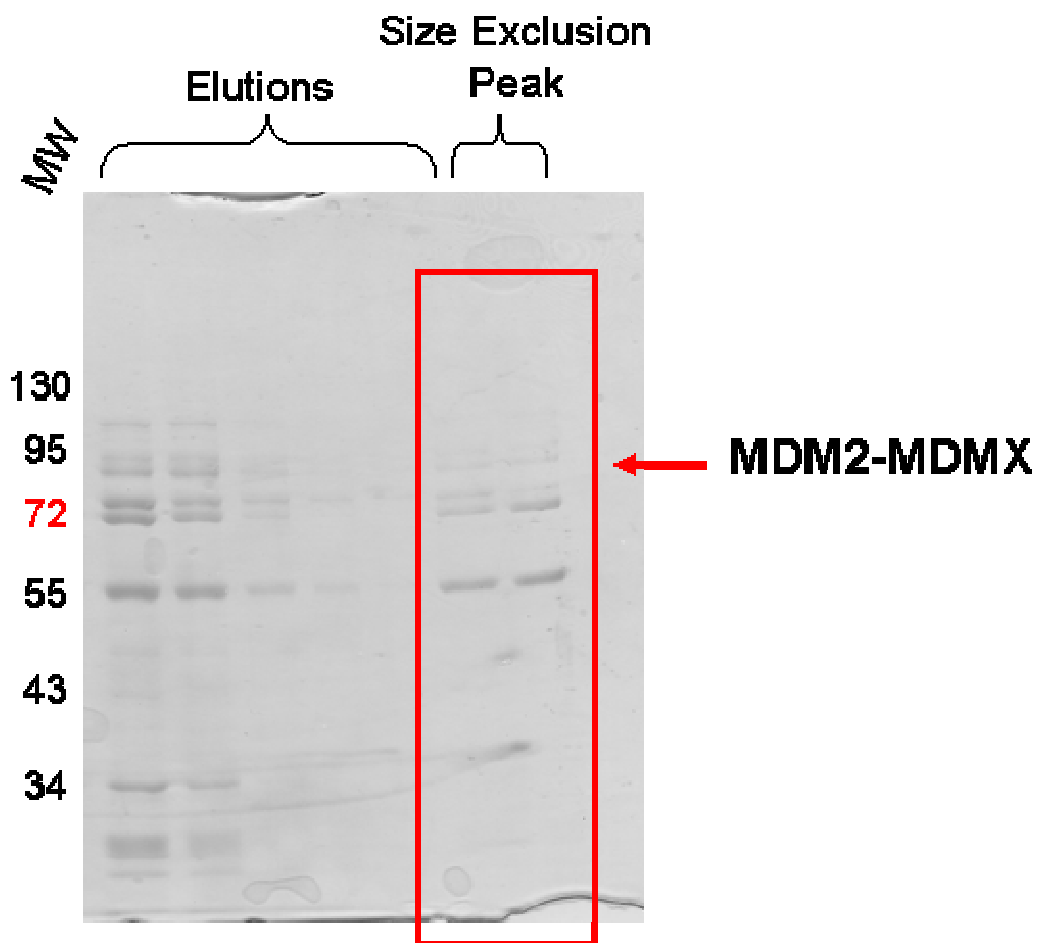
Figure 2.8. SDS-PAGE of Co-expressed MDM2-MDMX After Ni Affinity and Size Exclusion Chromatography Using High Salt Buffer Washes. Before, the Ni resin was washed with high salt (1 M NaCl) before eluting the protein using imidazole. According to the gel, many contaminants are present in the protein sample. Even though the elutions were subject to size exclusion chromatography, the elutions still contain many lower molecular weight contaminants.

a)
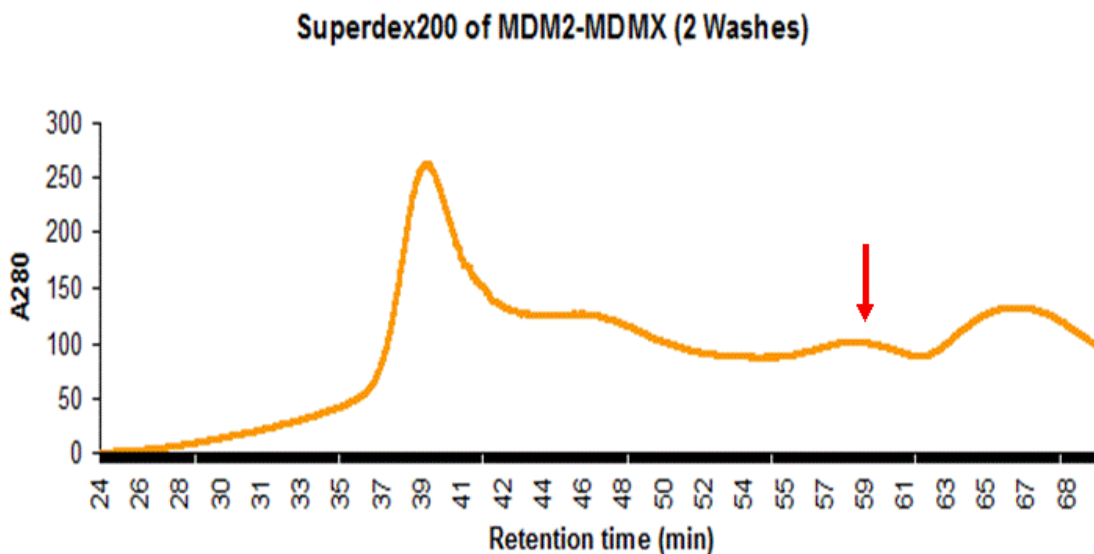
b)
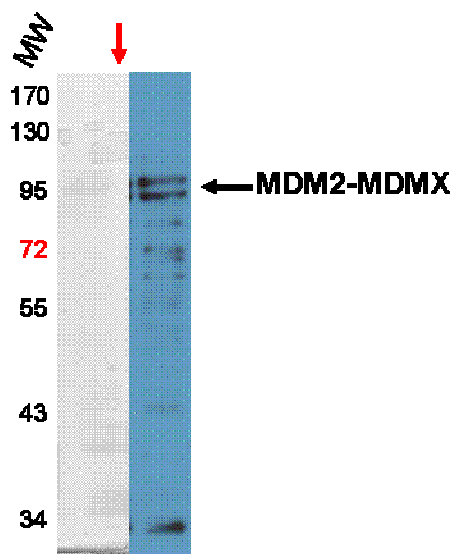
Figure 2.9. Size Exclusion Chromatography, SDS-PAGE, and Western Blot from Two Low Salt Buffer Washes. A) This chromatogram was produced after changing the washes (in Ni affinity chromatography) from high salt buffer washes to low salt buffer washes. The peak possibly containing the MDM2-MDMX heterodimer is noted by a red arrow. B) The red-arrowed peak from the chromatogram was collected for analysis via SDS-PAGE and Western blot. Compared to the gel in Figure 2.8, this gel shows a purer form of MDM2-MDMX with less contaminants.

a)

Superdex200 of MDM2-MDMX (3 Washes)
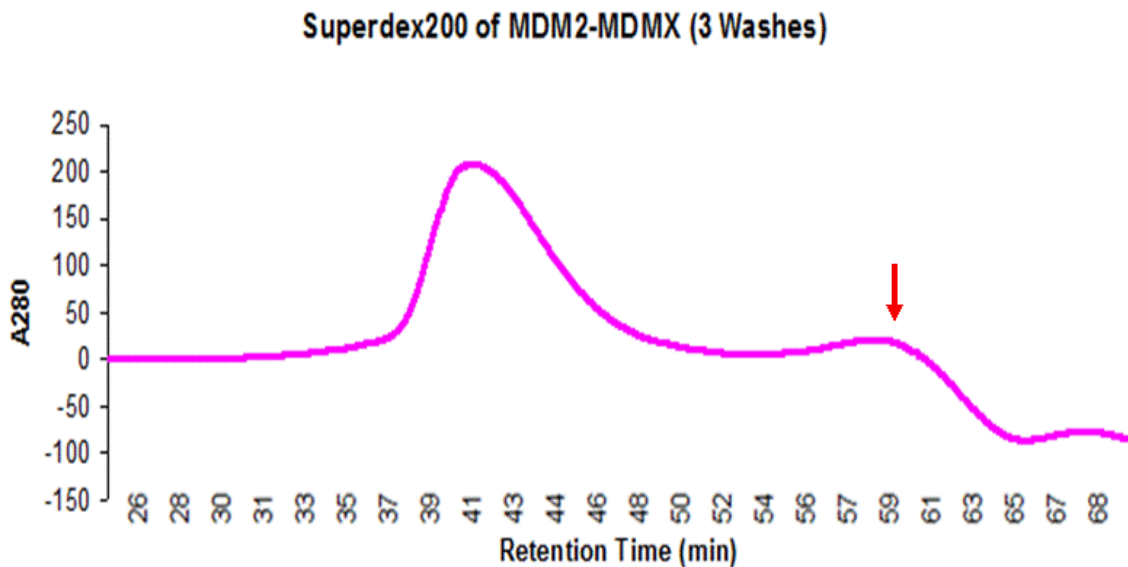
b)
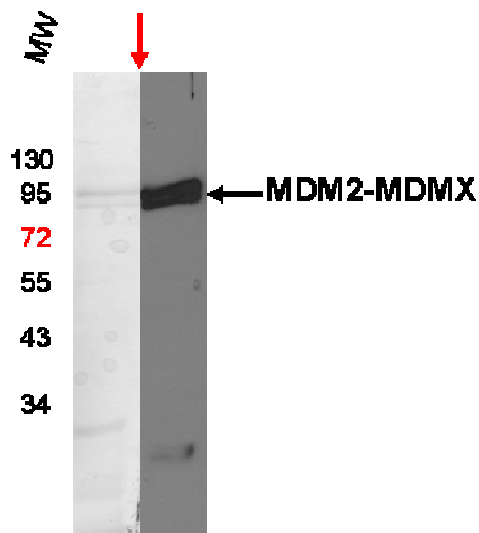
Figure 2.10. The Chromatogram and SDS-PAGE of Co-expressed MDM2-MDMX with Three Low Salt Washes. A) The chromatogram above was obtained after a prep was performed with three low salt washes in affinity chromatography. In comparison to the chromatogram in Figure 2.3, a peak at about 45.0 minutes is missing. B) A gel was run on the peak indicated by an arrow. According to the gel and the blot, the protein is present and is relatively pure.
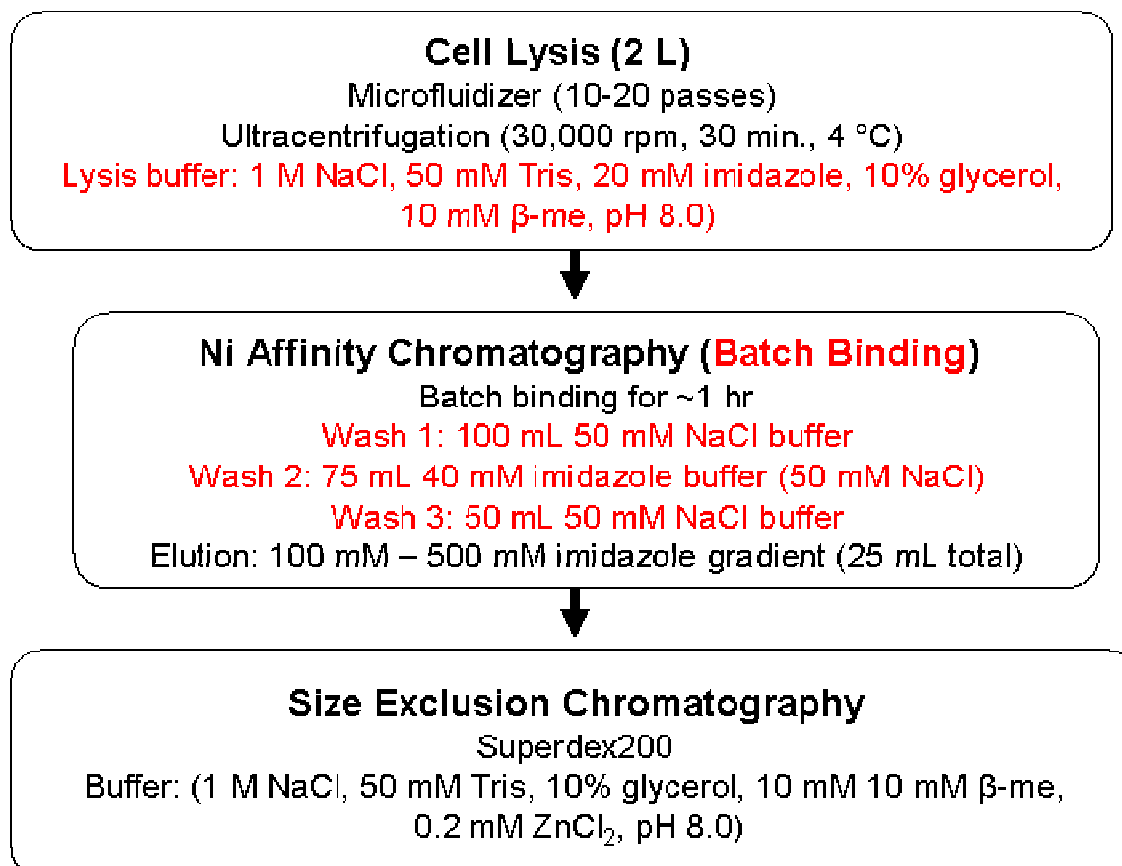
Figure 2.11. Optimized Purification Protocol for Co-expressed MDM2-MDMX. Here is a scheme of the optimized protocol, with the major points/changes noted in red. The lysis buffer (along with the elution and size exclusion buffers) includes high salt, glycerol, and β-me. The batch binding method is used for Ni affinity chromatography and the washes include low salt buffer.

a)

b)
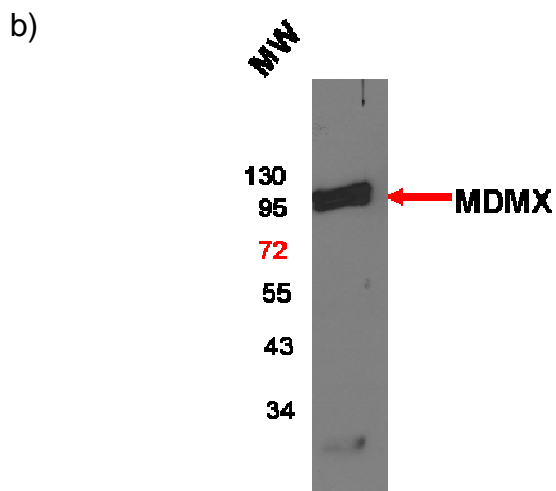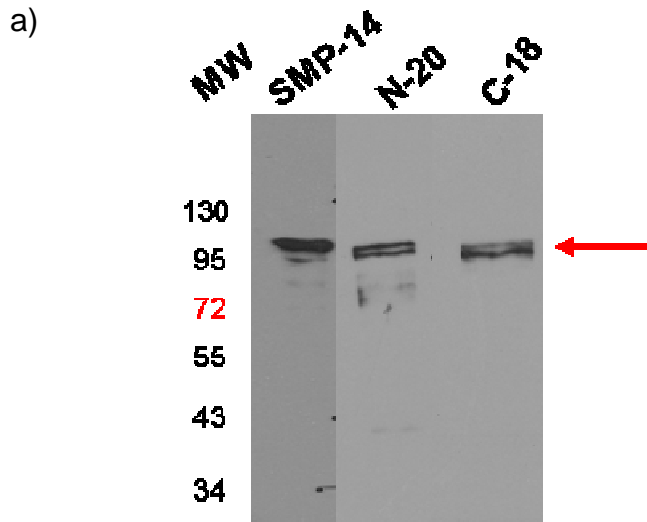
Figure 2.12. Western Blot using MDM2 Antibodies. A) In order to confirm MDM2's presence in the protein sample, a western blot was done using MDM2 (SMP-14, N-20, and C-18) antibodies. The MDM2 antibodies were incubated with the nitrocellulose membrane as primary antibodies, while the HRP antibodies were incubated as secondary antibodies in order to react with the ECL solution. According to the developed films, MDM2 is present in the sample. B) The presence of MDMX was assessed by using a His antibody since the MDMX gene was inserted into the polylinker containing a His-tag.

Table 2.1 Mass Spectrometry (Electrospray Ionization) Results
Dr. Majid Ghassemian performed an ESI experiment on an impure sample
(which was obtained when MDM2, MDMX, and p53 were co-purified) to validate
the presence of MDM2. The results are shown in the table below. According to
the results, MDM2 was present in the sample.

N	Unused	Total	%Cov	%Cov(50)	%Cov(95)	Name	Peptides(95%)
1	57.83	57.83	44.21	40.63	40.63	fused UDP-L-Ara4N =	43
2	29.54	29.54	48.36	35.07	34.93	chaperone Hsp70, co-chaperone with =	16
3	28.03	28.03	37.33	30.31	30.31	keratin 10 [Homo sapiens]	15
4	20.08	20.08	26.76	20.93	20.93	mouse double minute 2 homolog isoform MDM2 [Ho	14
5	18.3	18.3	35.37	31.55	28.5	tumor protein p53 [Homo sapiens]	12

DISCUSSION

The objective of this project was to successfully purify the MDM2-MDMX heterodimer. In order to obtain pure protein, many steps were taken to create an optimal purification protocol, which included the purification of the MDM2 and MDMX homo-oligomers, co-purification of MDM2-MDMX after individual expression, and the co-purification of the MDM2-MDMX complex from a single vector. According to the results, changes in the lysis buffer and the Ni affinity chromatography methods needed to be made to purify the MDM2-MDMX complex.

According to the purification research with pET28 MDM2, there was higher protein yield when the salt concentration of the buffer was increased from 500 mM to 1 M NaCl and when 10% glycerol was added. The higher yield may have been achieved due to the increase in protein solubility and stability due to the higher salt and glycerol. With those two components, more protein may have been rescued from the cell pellet during lysis; hence, leading to higher amounts of protein.

For Ni affinity chromatography, the use of the peristaltic pump led to the production of aggregates. Although the addition of β-me slightly alleviated the aggregation, the batch binding method produced higher protein yields probably due to the use of gravity when passing proteins instead of using an automated system. The multiple washes during Ni affinity chromatography also created a significant difference that is apparent when a size exclusion chromatography is run. According to the chromatograms and the SDS-PAGE gels, the multiple

washes with the low salt buffer diminished the amount of nonspecific binding onto the Ni column. Since the SDS-PAGE gel shows two prominent bands (representing MDM2 and MDMX) that signify pure protein, it can be assumed that the protein is pure enough for analysis under the electron microscope.

I would like to acknowledge Dr. Majid Ghassemian for taking my protein sample for analysis using Mass Spectrometry. Without his help, it would have been more difficult in determining the presence of the target proteins.

Chapter Three

Structural Studies of the MDM2-MDMX

Heterodimer

INTRODUCTION

The MDM2-MDMX interaction is important in understanding the individual proteins' functions. While p53 activity is diminished in cancers, MDM2 and MDMX activities are enhanced due to their over-expression (Terzian et al., 2007). Although these are two different proteins, studies have shown that MDM2 and MDMX are dependent on each other to perform efficiently as negative p53 regulators (Gu et al., 2002). MDMX depends on MDM2 for nuclear transport in order to function, for MDMX is inactivated in the cytoplasm (Gu et al., 2002). MDM2 on the other hand, relies on MDMX for stabilization and promotion of its E3 ubiquitin ligase activity (Gu et al., 2002). Considering how important they are to each others' activities, the relationship between the two proteins is crucial in p53 degradation.

However, the details and specific mechanisms of MDM2 and MDMX are obscure, for not many structural studies have been done on them. Therefore, the heterodimerization of MDM2 and MDMX via the C-terminal RING domains is a topic of interest in p53 research (Grier et al., 2006, Pant et al., 2011). Although the crystal structure of the MDM2-MDMX complex has been elucidated, that complex only contained the shared RING domains between the two proteins (Linke et al., 2008). This project focuses on the elucidation of the full-length MDM2-MDMX complex using the purified protein from the optimized purification protocol. The purified protein was later negatively stained and observed under the electron microscope for single particle analysis and reconstruction.

MATERIALS AND METHODS

Purification and Expression of MDM2-MDMX

The purification protocol for pETDUET MDM2-MDMX was optimized and is described in detail in the previous chapter. The sample from Figure 2.10 was used for electron microscopy.

Electron Microscopy (EM)

After carbon coating the copper grids, a glow-discharger was used to put charge onto the grids (to make them hydrophilic for sample binding). The sample of protein was diluted by 100-fold and about 4 µL of it was dropped onto the grid for a minute before it was washed with water drops. After washing the grid with water, a solution of uranyl acetate was used for negative staining. Once the grids were stained, they were ready for analysis under the microscope. The grids were observed digitally using a CM120 TEM with a CCD camera (at 110,000X magnification) in order to identify the appropriate grids to use for obtaining photographic images.

The FEI Sphera transmission electron microscope at 200 kV was used to obtain the photographic images at 0 and 60 degrees tilt (at 62,000X magnification, 25 Å, 1.5 µm defocus). The photographic images from the random conical tilt method were then scanned and later used for image processing. (Although I performed the initial scanning of the copper grids, the photographic films from the different microscope were obtained by Dr. Viadiu)

2D Image Refinement and 3D Reconstruction

Once the photographic films of the untilted and tilted particles were obtained, they were scanned using the Nikon SuperCoolScan9000 scanner. After the images were digitized, JWEB was used for particle selection. Once the particles were chosen, they were analyzed using SPIDER (System for Processing Image Data from Electron Microscopy and Related fields) for image processing. First, the untilted particles were used to create class averages. After specific class averages were determined for 3D reconstruction, the tilted particles matching the untilted particles were chosen to perform the back projection algorithm for 3D reconstruction.

RESULTS AND DISCUSSION

Analysis of a specimen under the microscope

After purifying the MDM2-MDMX heterodimer, many copper grids were prepared for observation under the electron microscope. Out of the many grids prepared, a few of them were successful in producing suitable images, for there is a distinction between the protein and the background (Figure 3.1). That same grid was then used to obtain tilted and untilted photographic images for 2D image processing and refinement (Figures 3.2 and 3.3).

Using SPIDER for 2D refinement

28 pairs of photographic films were collected after observing the specimen under the electron microscope. JWEB was used to select a total of 2006 particles from the 28 pairs of film. After particle selection from the untilted and tilted images, the defective particles were deleted, creating a new total of 1942 particles. The particles from the untilted images were then used to create class averages. Some of the raw images of the untilted particles are shown in Figure 3.4. Using SPIDER, class averages were produced to observe stacked images of possible MDM2-MDMX heterodimers. In comparison to raw images, the class averages produced more defined images due to the compilation of many particles (Figure 3.5). Groups of 50, 16, and 10 class averages were observed using SPIDER. The averages for the 50 groups were created using a 27 pixel radius, while the averages for groups 10 and 16 were created using a 22 pixel radius. Nonetheless, for each of the groups, a dumbbell-shaped protein was

observed for at least one of the sets of averages (Figure 3.6). Since the dumbbell-shaped particle may represent the binding of MDMX and MDM2 monomers to create a heterodimer, we attempted to compile the particles creating that shape for 3D reconstruction. One of the class averages from the 10 groups was chosen for reconstruction. A total of 146 particles were used.

3D reconstruction of the heterodimer

In order to produce a 3D model of the MDM2-MDMX heterodimer, back projections of the tilted particles were calculated. When particle selection was done using JWEB, the angles of each particle were saved to use that information for 3D reconstruction. By compiling all of the angle information from the chosen tilted particles, a 3D model of the heterodimer can be created (Figure 3.7). After performing the back projection algorithm from the 146 tilted particles using SPIDER, a 3D representation of the MDM2-MDMX heterodimer was created (Figure 3.8). In comparison to the 2D image (from one of the 50 group class averages), the 3D model also consists of a dumbbell-shape. The 3D heterodimer was observed at different angles as well (Figure 3.9). Although the dumbbell-shape is preserved, the model looks relatively flat from the side, probably due to the fact that only 146 particles were used for reconstruction. In order to produce a more accurate image, it would be necessary to compile more particles for refinement.

Figure 3.1. EM Image of MDM2-MDMX at 0 Degrees. This photographic image was obtained using an electron microscope. After loading the specimen, the sample was analyzed at 200kV at 62kX magnification. Considering how there are clear distinctions between proteins and the background (proteins being white, while the rest is gray/black), this specimen was used for obtaining more images for particle selection.
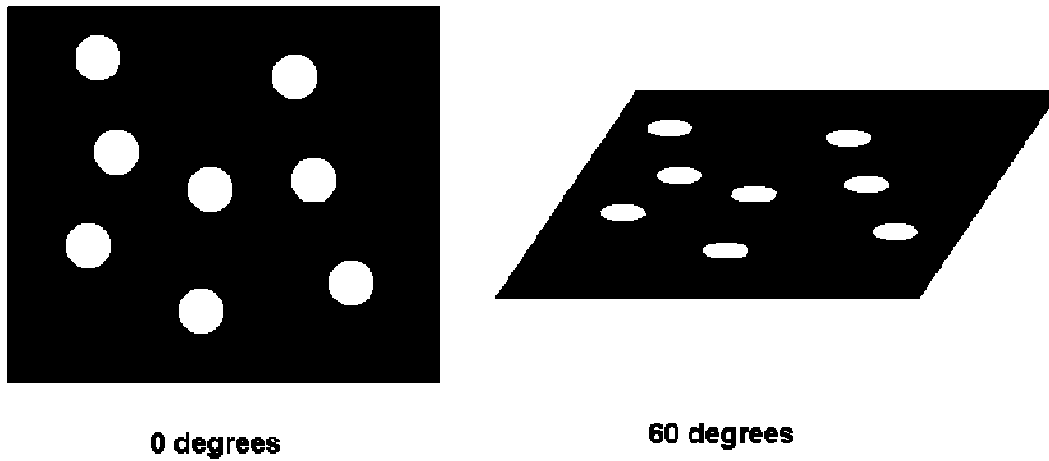
0 degrees   **60 degrees**

Figure 3.2. Tilted Versus Untilted Images. The image above represents the differences between an image taken at 0 degrees and 60 degrees. The proteins are shown as white circles while the black portion is the background. It is expected for proteins to look flat when the specimen is viewed at no tilt. At a 60 degree tilt, the particles look distorted and angular. By taking pairs of images in a 0 degree and 60 degree tilt, the information from both of them can be used later for 2D and 3D refinement.

a)

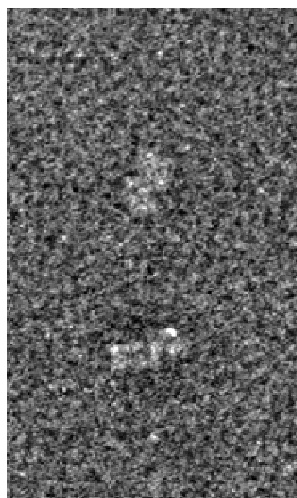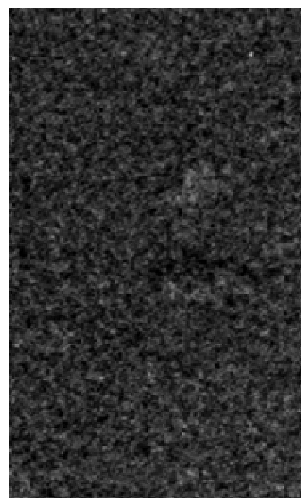**Untilted**   **Tilted**

b)

Untilted   **Tilted**

Figure 3.3. Photographic Images of Tilted and Untilted MDM2-MDMX. A) This pair of images show the untilted and tilted portions of the same regions. While the untilted image looks flatter, the tilted image is more skewed. B) Another pair of images was used to take a closer look at the differences between untilted and tilted images. Two particles are seen in the untilted image, which is also seen in the tilted image. However, the particles in the tilted image are distorted due to the 60 degree tilt.
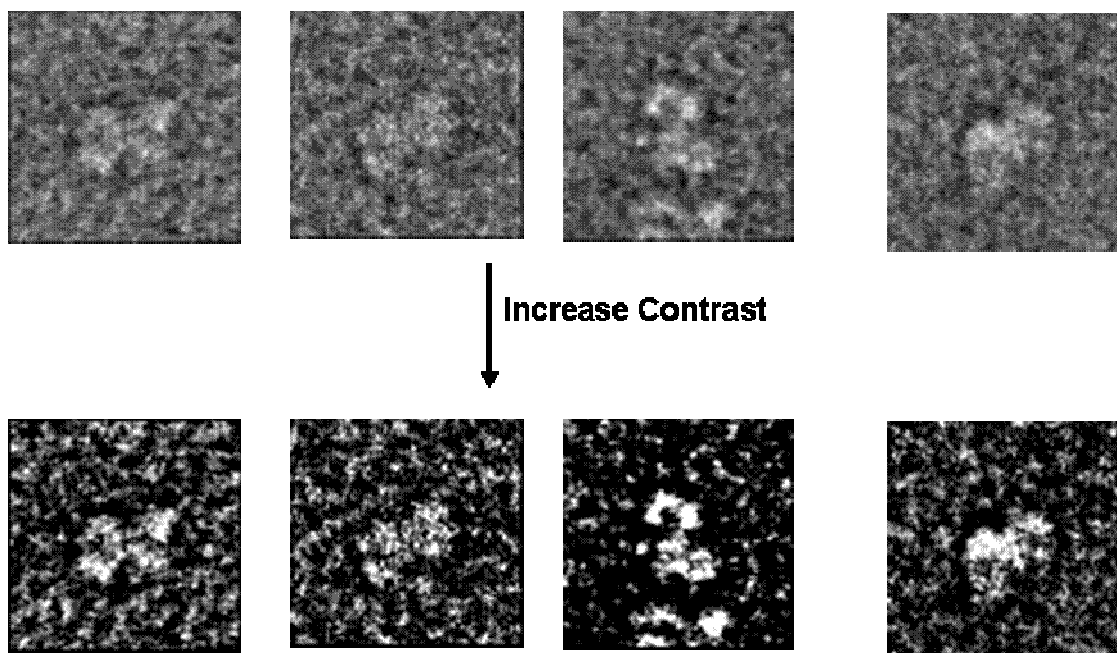
Figure 3.4.   Raw Images of Untilted Particles.   In order to produce class averages, raw images of the untilted particles had to be chosen.   This figure shows examples of some of the raw, untilted images that were chosen using JWEB.   The contrast was adjusted in order to observe the particles with more ease.
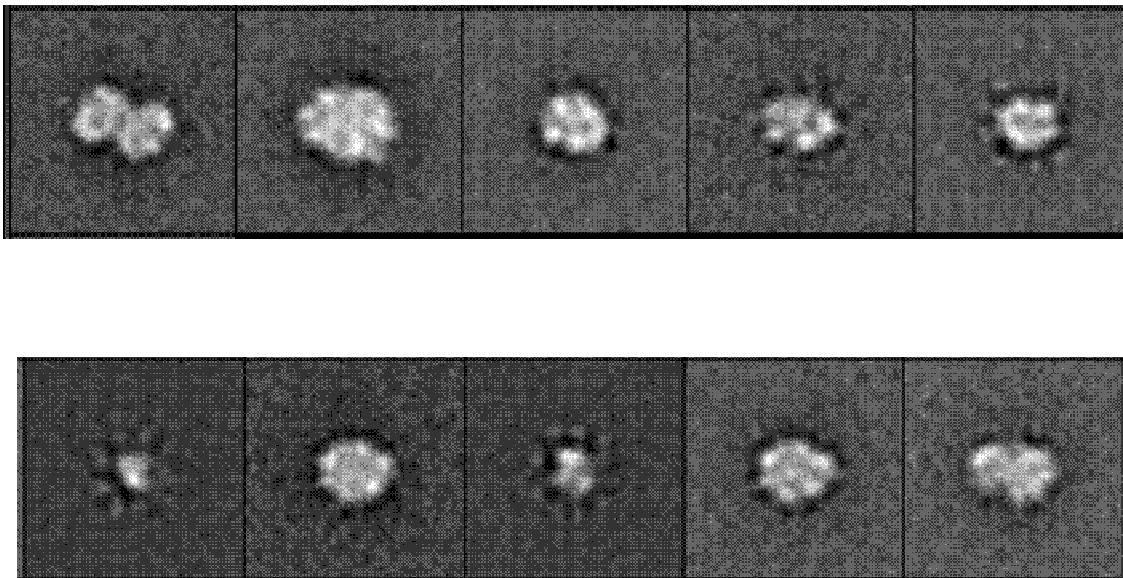
Figure 3.5. Averages of the Untilted Particles. SPIDER was used to classify the particles to produce class averages. This figure shows 8 out of 16 class averages that were created (with a 22 pixel radius). Compared to the raw images, the class averages are clearer and more defined.
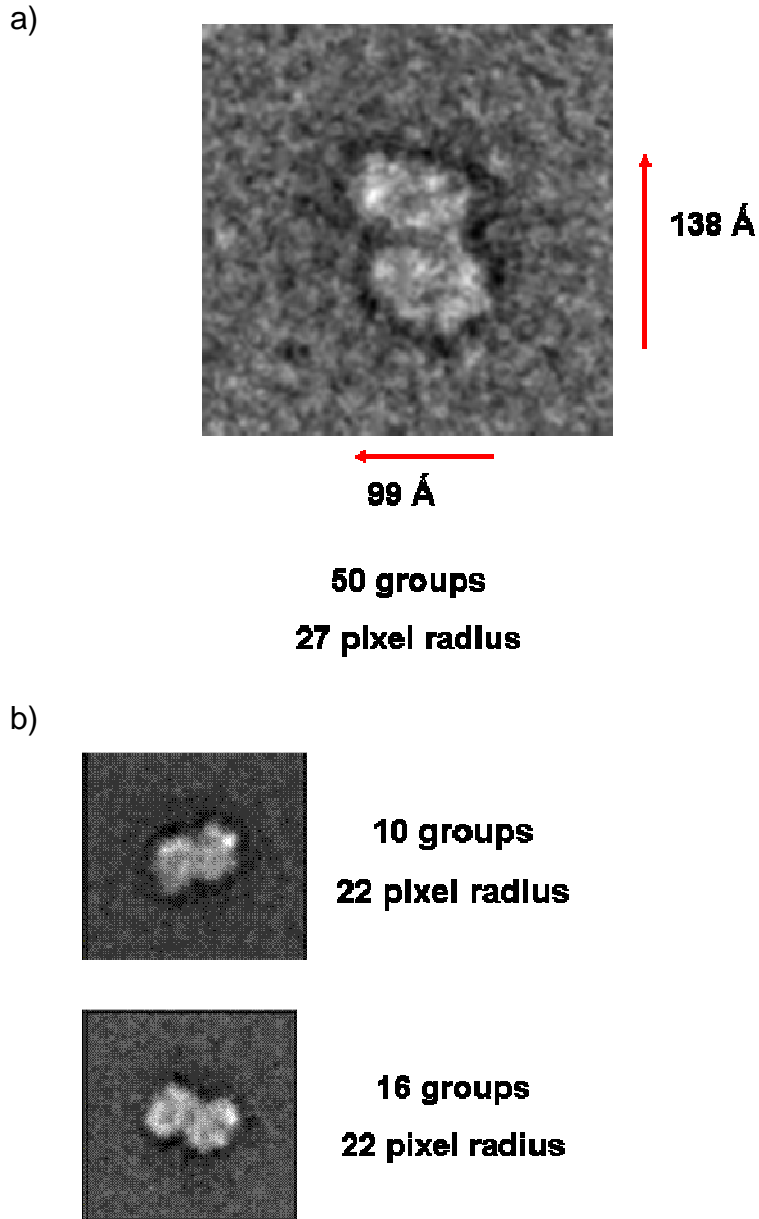
a)

138 Å

99 Å

50 groups
27 pixel radius

b)

10 groups
22 pixel radius

16 groups
22 pixel radius

Figure 3.6. Averages Indicating the MDM2-MDMX Heterodimer. A) When 50 class groups (averages with a 27 pixel radius) were produced, a few of the groups consisted of a dumbbell-shaped particle, which may signify the heterodimer. B) Less class averages were created to determine if the dumbbell-shaped particle gets distorted. When 10 groups and 16 groups were created with a 22 pixel radius, one of the averages from the two groups contained a dumbbell-shaped particle.
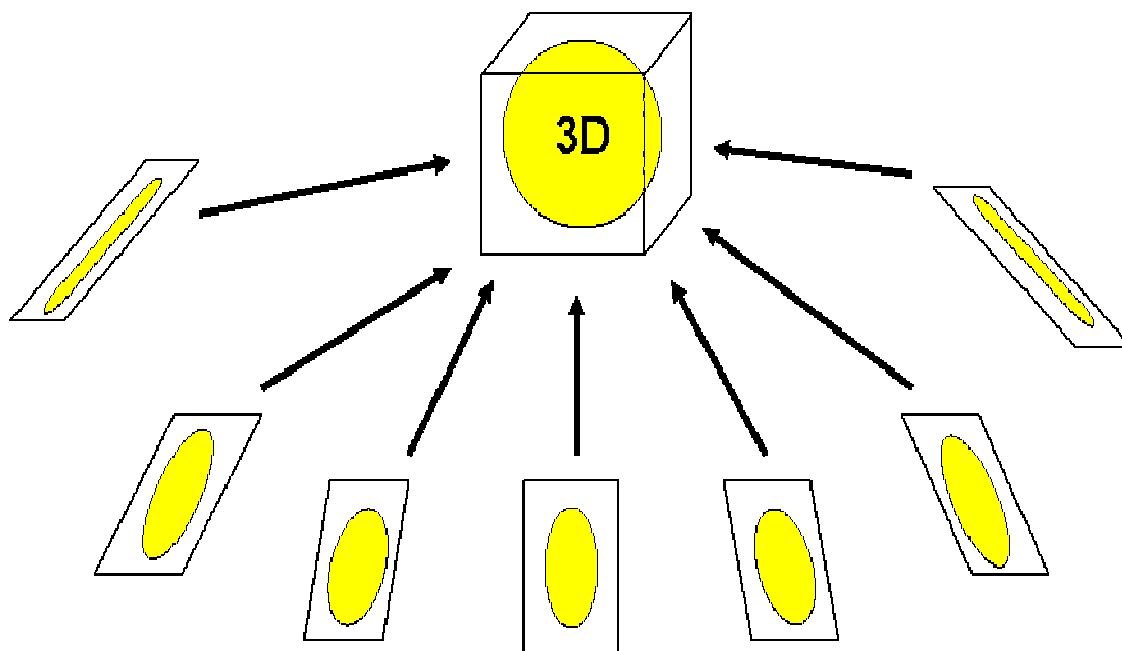
Figure 3.7. Representation of Back Projection. After obtaining the class averages from the untilted particles, tilted particles corresponding to the untilted particles were subject to back projection. Back projection involves an algorithm that uses angular information from the tilted particles. When the tilted particles were chosen in JWEB, the angle information was retained. That information is then translated to create a 3D representation of the molecule.
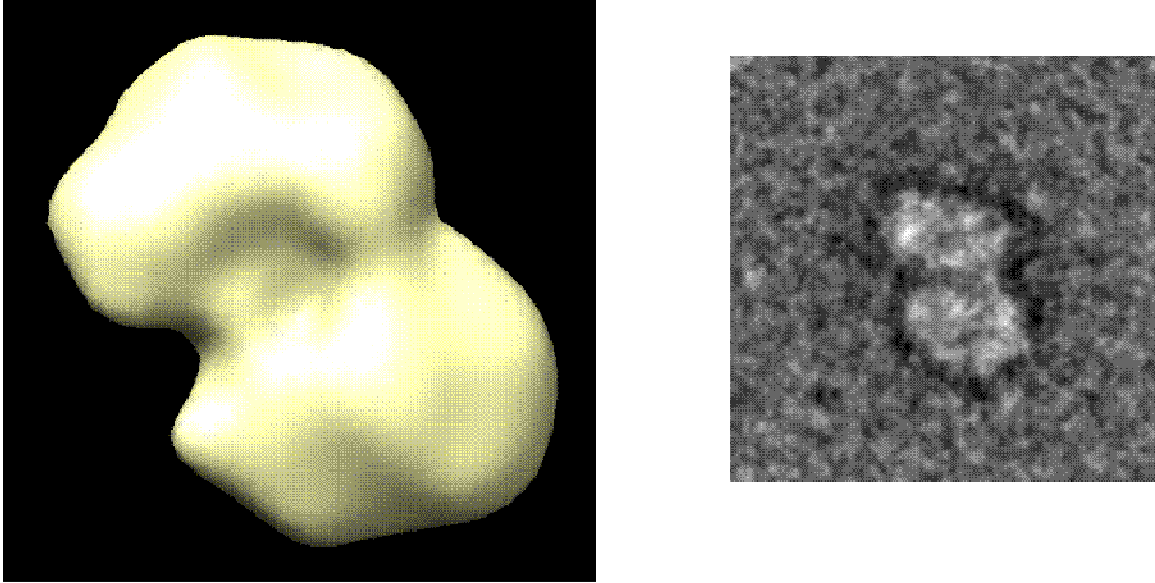
Figure 3.8. 3D and 2D Representation of the MDM2-MDMX Heterodimer.
After the back projection algorithm was performed using 146 particles, a 3D model of the heterodimer was created. One of the class averages (50 groups, 27 pixel radius) is shown next to it to compare the 2D and 3D representations. According to the 3D model, the two images are both composed of a dumbbell-shaped particle.

Figure 3.9. Different Views of the 3D MDM2-MDMX Heterodimer. Images of the 3D heterodimer are shown at different angles. More particles may be used next time for further refinement.

References

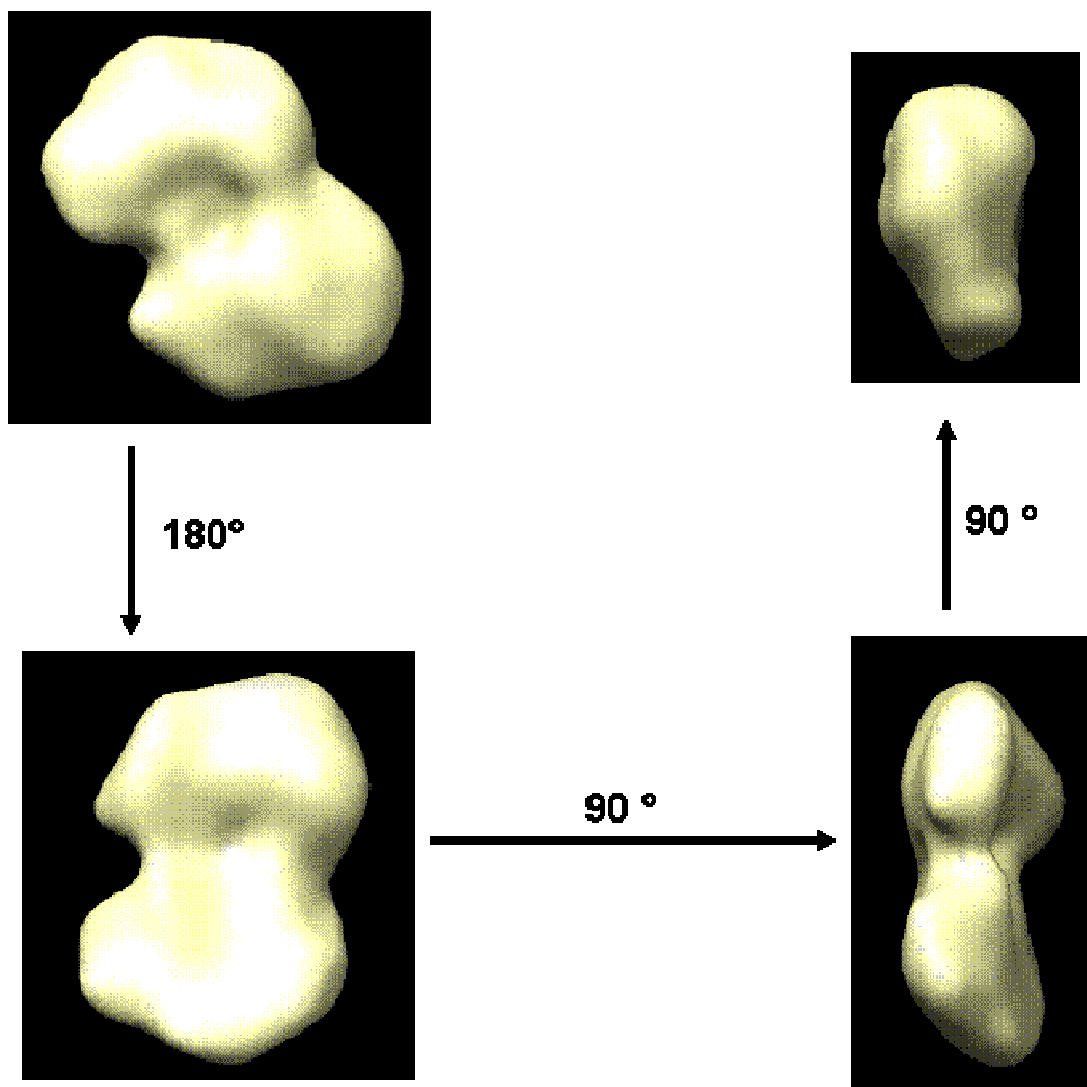Bai, L., and W. Zhu. "p53: Structure, Function and Therapeutic Applications." Journal of Cancer Molecules 2.4 (2006): 141-153.

Blanco, E., X.Messeguer, T.F. Smith, and R. Giugo. "Transcription Factor Map Alignment of Promoter Regions." *PLoS Computational Biology* 2.5 (2006).

Brooks, Christopher L., and Wei Gu. "p53 Ubiquitination: Mdm2 and Beyond." *Molecular Cell* 21.3 (2006): 307-315.

Chene, P.. "Inhibiting The p53-MDM2 Interaction: An Important Target for Cancer Therapy." *Nature Reviews. Cancer.* 3.2 (2003): 102-109.

Cheung, N. H. L. "Biophysical Characterization of p53 regulatory domain and MDM2." University of California, San Diego (2010).

Cross, B., L. Chen, Q. Cheng, B. Li, Z. Yuan, and J. Chen. "Inhibition of p53 DNA Binding Function by the MDM2 Acidic Domain." *The Journal of Biological Chemistry* 286.18 (2011): 16018-16029.

Deisenroth, C., and Y. Zhang. "The Ribosomal Protein-Mdm2-p53 Pathway and Energy Metabolism: Bridging the Gap between Feast and Famine." *Genes & Cancer* 2.4 (2011): 392-403.

Dolezelova, P., K. Cetkovska, K.H. Vousden, and S. Ulrijan. "Mutational analysis reveals a dual role of Mdm2 acidic domain in the regulation of p53 stability." *FEBS Letters* 586.16 (2012): 2225-2231.

Ethayathulla, A.S., P. Tse, P. Monti, S. Nguyen, A. Inga, G. Fronza, and H. Viadiu. "Structure of p73 DNA-binding domain tetramer modulates p73 transactivation." *PNAS* 109.16 (2011): 6066-6071.

Fang, S., J.P. Jensen, R.L. Ludwig, K.H. Vousden, and A.M. Weissman. "Mdm2 Is a RING Finger-dependent Ubiquitin Protein Ligase for Itself and p53." *The Journal of Biological Chemistry* 275.12 (1999): 8945-8951.

Francoz, S., P. Froment, S. Bogaerts, S. De Clercq, M. Maetens, G. Doumont, E. Bellefrold, and J. Marine. Mdm4 and Mdm2 cooperate to inhibit p53 activity in proliferating and quiescent cells *in vivo.*" *PNAS* 103.9 (2006): 3232-3237.

Graves, B., T. Thompson, M. Xia, C. Janson, C. Lukacs, D. Deo, P. Di Leo, D.Fry, C. Garvie, K. Huang, L. Gao, C. Tovar, A. Lovey, J. Wanner, and L.T. Vassilev. "Activation of the p53 pathway by small-molecule-induced MDM2 and MDMX dimerization." *PNAS* 109.29 (2012): 11788-11793.

Grier, J.D., S. Xiong, A.C. Eizondo-Fraire, J.M. Parant, and G. Lozano. "Tissue-Specific Differences of p53 Inhibition by Mdm2 and Mdm4." *Molecular and Cellular Biology* 26.1 (2006): 192-198.

Gu, J., H. Kawai, L. Nie, H. Kitao, D. Wiederschain, A.G. Jochemsen, J. Parant, G. Lozano, and Z. Yuan. Mutual Dependence of MDM2 and MDMX in Their Functional Inactivation of p53." *The Journal of Biological Chemistry* 277.22 (2002): 19251-19254.

Huang, L., Z. Yan, X. Liao, Y. Li, J. Yang, Z. Wang, Y. Zuo, H. Kawai, M. Shadfan, S. Ganapathy, and Z. Yuan. "The p53 inhibitors of MDM2/MDMX complex is required for control of p53 activity in vivo." *PNAS* 108.29 (2011): 12001-12006.

Iwakuma, T., and G. Lozano. "MDM2, An Introduction." *Molecular Cancer Research* 1.14 (2003): 993-1000.

Inga, A., F. Storici, T.A. Darden, and M.A. Resnick. "Differential transactivation by the p53 transcription factor is highly dependent on p53 level and promoter target sequence." *Molecular and Cellular Biology* 22.24 (2002): 8612-8625.

Kim, S. K. "Structural and Functional Characterization of the p53 C-terminus". University of California, San Diego (2012).

Kostic, M., T. Matt, M.A. Martinez-Yamout, H.J. Dyson, P.E. Wright. "Solution structure of the Hdm2 C2H2C4 RING, a domain critical for ubiquitination of p53." Journal of Molecular Biology 363.2 (2006): 433-450.

Kulikov, R., M. Winter, and C. Blattner. "Binding of p53 to the Central Domain of Mdm2 Is Regulated by Phosphorylation." *The Journal Of Biological Chemistry* 281.39 (2006): 28575-28583.

Kussie, P.H., S. Gorina, V. Marechal, B. Elenbaas, J. Moreau, A.J. Levine, and N.P. Pavletich. "Structure of the MDM2 oncoprotein bound to the p53 tumor suppressor transactivation domain." Science 274.5289 (1996): 948-953.

Lindstrom, M.S., A. Jin, C. Deisenroth, G. White Wolf, and Y. Zhang. "Cancer-Associated Mutations in the MDM2 Zinc Finger Domain Disrupt Ribosomal Protein Interaction and Attenuate MDM2-Induced p53 Degradation." *Molecular and Cellular Biology* 27.3 (2007): 1056-1068.

Linke, K., P.D. Mace, C.A. Smith, D.L. Vaux, J. Silke, and C.L. Day. "Structure of

the MDM2/MDMX RING domain heterodimer reveals dimerization is required for their ubiquitylation in *trans*." *Cell Death and Differentiation* 15.5 (2008): 841-848.

Lommel, L., S.M. Gregory, K.I. Becker, and K.S. Sweder. "Transcription-coupled DNA repair in yeast transcription facot IIE (TFIIE) mutants." *Nucleic Acids Research* 28.3 (2000): 835-842.

Malek, R., J. Matta, N. Taylor, M.E. Perry, and S.M. Mendrysa. "The p53 Inhibitor MDM2 Facilitates Sonic Hedgehog-Mediated Tumorigenesis and Influences Cerebellar Foliation." *PLoS ONE* 6.3 (2011): e17884.

McCoy, M.A., J.J. Gesell, M.M. Senior, and D.F. Wyss. "Flexible lid to the p53-binding domain of human Mdm2: Implications for p53 regulation." *PNAS* 100.4 (2003): 1645-1648.

Melo, A.N., and C.M. Eischen. "Protecting the Genome from Mdm2 and Mdmx." *Genes & Cancer* 3.3-4 (2012): 283-290.

Moll, U.M., and O. Petrenko. "The MDM2-p53 Interaction." *Molecular Cancer Research* 1 (2003): 1001-1008.

Pant, V., S. Xiong, T. Iwakuma, A. Quintas-Cardama, and G. Lozano. "Heterodimerization of Mdm2 and Mdm4 is critical for regulating p53 activity during embryogenesis but dispensable for p53 and Mdm2 stability." *PNAS* 108.29 (2011): 11995-12000.

Poyurovsky, M.V., C. Priest, A. Kentsis, K. LB Borden, Z. Pan, N. Pavletich, and C. Prives. "The Mdm2 RING domain C-terminus is required for supramolecular assembly and ubiquitin ligase activity." *The EMBO Journal* 26.1 (2007): 90-101.

Priest, C., C. Prives, and M.V. Poyurovsky. "Deconstructing nucleotide binding activiy of the Mdm2 RING domain." *Nucleic Acids Research* 38.21 (2010): 7587-7598.

Ranaweera, R.S., and X. Yang. "Auto-ubiquitination of Mdm2 enhances its substrate ubiquitin activity." *Journal of Biological Chemistry* (2013).

Rew, Y., D. Sun, F. Gonzalez-Lopez De Turiso, M.D. Bartberger, H.P. Beck, J. Canon, A. Chen, D. Chow, J. Deignan, B.M. Fox, D. Gustin, X. Huang, M. Jiang, X. Jiao, L. Jin, F. Kayser, D.J. Kopecky, Y. Li, M. Lo, A.M. Long, K. Michelsen, J.D. Oliner, T. Osgood, M. Ragains, A.Y. Saik, S. Schneider, M. Toteva, P. Yakowec, X. Yan, Q. Ye, D. Yu, X. Zhao, J. Zhou, J.C. Medina, and S.H. Olson. "Structure-Based Design of Novel Inhibitors of

the MDM2-p53 Interaction." *Journal of Medicinal Chemistry* 55.11 (2012): 4936-4954.

Sakaguchi, K., J.E. Herrera, S. Saito, T. Miki, M. Bustin, A. Vassilev, C.W. Anderson, and E. Appella. "DNA damage activates p53 through a phosphorylation-acetylation cascade." Genes and Development 12.18 (1998): 2831-2841.

Sasaki, M., K. Kawahara, M. Nishio, K. Mimori, R. Kogo, K. Hamada, B. Itoh, J. Wang, Y. Komatsu, Y. R. Yang, H. Hikasa, Y. Horie, T. Yamashita, T. Kamijo, Y. Zhang, Y. Zhu, C. Prives, T. Nakano, T.W. Mak, T. Sasaki, T. Maehama, M. Mori, and A. Suzuki. "Regulation of the MDM2-P53 pathway and tumor growth by PICT1 via nucleolar RPL11." *Nature Medicine* 17.8 (2011): 944-951.

Shan, B., D. Li, L. Bruschweiler-Li, and R.I Bruschweiler. "Competitive Binding between Dynamic p53 Transactivation Subdomains to Human MDM2 Protein." *The Journal of Biological Chemistry* 287.36 (2012): 30376-30384.

Stad, R., N.A. Little, D.P. Xirodimas, R. Frenk, A.J. van der Eb, D.P. Lane, M.K. Saville, and A.G. Jochemsen. "Mdmx stabilizes p53 and Mdm2 via two distinct mechanisms." *EMBO Reports* 2.11 (2001): 1029-1034.

Sun, J., H. Viadiu, A.K. Aggarwal, and H. Weinstein. "Energetic and structural considerations for the mechanism of protein sliding along DNA in the nonspecific BamHI-DNA complex." Biophysical Journal 84.5 (2003): 3317-3325.

Tanimura, S., S. Ohtsuka, K. Mitsui, K. Shirouzu, A. Yoshimura, M., Ohtsubo. "MDM2 interacts with MDMX through their RING finger domains." *FEBS Letters* 447.1 (1999): 5-9.

Terzian, T., Y. Wang, C.S. Van Pelt, N.F. Box, E.L. Travis, and G. Lozano. "Haploinsufficiency of *Mdm*2 and *Mdm*4 in Tumorigenesis and Development." *Molecular and Cellular Biochemistry* 27.15 (2007): 5479-5485.

Toledo, F., and G.M. Wahl. "MDM2 and MDM4: p53 regulators as targets in anticancer therapy." *Journal of Biochemistry Cell Biology* 39.7-8 (2008): 1476-1482.

Wade, M., Y.V. Wang, and G.M. Wahl. "The p53 orchestra: Mdm2 and Mdmx set the tone." *Trends in Cell Biology* 20.5 (2010): 299-309.

Wasserman, W.W., and W.E. Fahl. "Functional antioxidant responsive elements." *PNAS* 94.10 (1997): 5361-5366.

Xiong, S., C.S. Van Pelt, A.C. Elizaondo-Fraire, G. Liu, a nd G. Lozano. "Synergistic roles of Mdm2 and Mdm4 for p53 inhibition in central nervous system development." PNAS 103.9 (2006): 3226-3231.

Yu, G.W., M.D. Allen, A. Andreeva, A.R. Fersht, and M. Bycroft. "Solution structure of the C4 zinc finger domain of HDM2." Protein Science 15.2 (2006): 384-349.

Zaret, K.S., and J.S. Carroll. "Pioneer transcription factors: establishing competence for gene expression." *Genes and Development* 25.21 (2011): 2227-2241.